Old Dominion University
ODU Digital Commons

OEAS Faculty Publications | Ocean, Earth & Atmospheric Sciences

2021

Salt Marsh Hydrogeology: A Review

Julia Guimond

Joseph Tamborski
Old Dominion University, jtambors@odu.edu

Follow this and additional works at: https://digitalcommons.odu.edu/oeas_fac_pubs

 Part of the Geology Commons, Hydrology Commons, and the Oceanography Commons

Original Publication Citation

Guimond, J., & Tamborski, J. (2021). Salt marsh hydrogeology: A review. *Water, 13*(4), 1-23, Article 543. https://doi.org/10.3390/w13040543

This Article is brought to you for free and open access by the Ocean, Earth & Atmospheric Sciences at ODU Digital Commons. It has been accepted for inclusion in OEAS Faculty Publications by an authorized administrator of ODU Digital Commons. For more information, please contact digitalcommons@odu.edu.

water

MDPI

Review

Salt Marsh Hydrogeology: A Review

Julia Guimond [1,2,*] and Joseph Tamborski [3]

[1] Department of Civil and Resource Engineering, Dalhousie University, Halifax, NS B3H 4R2, Canada
[2] Department of Geological Sciences, University of Delaware, Newark, DE 19716, USA
[3] Department of Ocean and Earth Sciences, Old Dominion University, Norfolk, VA 23529, USA; jtambors@odu.edu
* Correspondence: Julia.Guimond@dal.ca

Abstract: Groundwater–surface water exchange in salt marsh ecosystems mediates nearshore salt, nutrient, and carbon budgets with implications for biological productivity and global climate. Despite their importance, a synthesis of salt marsh groundwater studies is lacking. In this review, we summarize drivers mediating salt marsh hydrogeology, review field and modeling techniques, and discuss patterns of exchange. New data from a Delaware seepage meter study are reported which highlight small-scale spatial variability in exchange rates. A synthesis of the salt marsh hydrogeology literature reveals a positive relationship between tidal range and submarine groundwater discharge but not porewater exchange, highlighting the multidimensional drivers of marsh hydrogeology. Field studies are heavily biased towards microtidal systems of the US East Coast, with little global information available. A preliminary estimate of marsh porewater exchange along the Mid-Atlantic and South Atlantic Bights is 8–30 $\times$ 10^{13} L y^{-1}, equivalent to recirculating the entire volume of seawater overlying the shelf through tidal marsh sediments in ~30–90 years. This review concludes with a discussion of critical questions to address that will decrease uncertainty in global budget estimates and enhance our capacity to predict future responses to global climate change.

Keywords: salt marshes; groundwater–surface water exchange; submarine groundwater discharge; coastal wetlands; porewater exchange

check for updates

Citation: Guimond, J.; Tamborski, J. Salt Marsh Hydrogeology: A Review. *Water* **2021**, *13*, 543. https://doi.org/10.3390/w13040543

Academic Editor: Carlos Duque

Received: 15 December 2020
Accepted: 9 February 2021
Published: 20 February 2021

Publisher's Note: MDPI stays neutral with regard to jurisdictional claims in published maps and institutional affiliations.

Copyright: © 2021 by the authors. Licensee MDPI, Basel, Switzerland. This article is an open access article distributed under the terms and conditions of the Creative Commons Attribution (CC BY) license (https://creativecommons.org/licenses/by/4.0/).

1. Introduction

Salt marshes are often overlooked through the lens of groundwater–surface water interactions due to the low permeability of marsh sediments. While a large body of literature exists on groundwater–surface water exchange in the coastal zone [1–3], groundwater–surface water exchange in salt marshes is understudied compared to beach and nearshore environments. To this end, tidal marsh hydrogeology has recently been highlighted as a critical knowledge gap in the field [3] and has received renewed attention for its role in mediating chemical exports to the coastal ocean [4–6].

Salt marshes, a subset of coastal wetlands, are fine-grained intertidal ecosystems located along shorelines ranging from ocean margins to the freshwater–seawater interface. Generally, salt marshes consist of a surface unit of organic-rich, low permeability peat, mud, and clay that overtops sandy estuarine sediments, and are therefore distinct from sand-dominated beach environments. The marsh sediment depth varies depending on age, energy regime, and geologic history [7]. These periodically inundated peat- or mud-rich deposits and the area that they encompass are referred to as the marsh platform and are often incised by tidal creeks and channels that act as conduits to the coastal ocean [8]. Salt marshes occur across a range of tidal regimes (i.e., microtidal to megatidal) and geomorphological settings (e.g., restricted-entrance embayment, open coast back-barrier, fringing) [9,10]. Contributing to or stemming from these hydrological and geomorphological characteristics, a diversity of salt- and/or saturation-tolerant plant species colonize marsh platforms including *Spartina alterniflora* and *Spartina patens*.

Rates of groundwater–surface water exchange in salt marshes can greatly exceed inner shelf and beach environments [11], in part due to the unique permeability structure and geometry of marsh ecosystems. Vegetation (rhizomes and roots) [12], bioturbating organisms [13,14], sandy lenses [15] and macropore structures [16] collectively enhance the effective permeability of otherwise muddy, impermeable marsh sediments. Tidal creeks, and thus the creek network type, can enhance the effective area of groundwater–surface water exchange [17]. Marsh sediments and pore waters are frequently enriched in nutrients [18] and carbon [19] relative to coarser-grained systems (i.e., beaches) and have been shown to export vast quantities of carbon and nutrients into tidal creeks and the coastal ocean [20,21].

The idea that salt marshes export carbon and nutrients to the coastal ocean is the basis of the outwelling hypothesis, which states that salt marshes outwell excess organic matter, dissolved carbon and nutrients to tidal channels, estuaries and the coastal ocean via tidal drainage and exchange [22,23]. Initially, the outwelling discussion was largely centered around nutrient (and predominantly nitrogen) fluxes [20,24–26]. Recent advances in blue carbon science have linked salt marshes to regional carbon budgets [5,27,28], thus renewing interest in the outwelling hypothesis. While salt marsh biogeochemistry mediates the quantity and form of nutrients and carbon [29], the magnitude of groundwater–surface water exchange will ultimately drive removal (internal consumption or adsorption onto sediments) or lateral export (i.e., outwelling). Thus, the quantification of salt marsh groundwater–surface water exchange is critical to understand interecosystem variability, and to accurately upscale fluxes between local, regional and global scales.

To this end, we focus this review on groundwater–surface water exchange in salt marshes, excluding other coastal vegetated ecosystems such as mangroves and seagrass beds. This review starts with a discussion of terminology, given recent changes and suggestions from both hydrogeologic and oceanographic communities. We then transition to a discussion of drivers and patterns of water exchange and the suite of methods used to quantify them. Synthesizing the salt marsh hydrogeology literature, we discuss outstanding questions and recommendations for future research endeavors.

2. Defining Groundwater–Surface Water Exchange and Zonation in Salt Marshes

The exchange of groundwater to surface water in coastal environments is termed submarine groundwater discharge (SGD), which is defined as "any and all flow of water on continental margins from the seabed to the coastal ocean, regardless of fluid composition or driving force" [30]. SGD is often deconstructed and delineated into groundwater discharge and porewater exchange (PEX) flow paths, yet this delineation is inconsistent across studies. For example, pioneering studies on salt marsh hydrogeology differentiated between groundwater discharge from the underlying aquifer and porewater drainage from the marsh soils [31–34]. This delineation based on hydrostratigraphic units contrasts with the currently accepted definitions of SGD and PEX, in which the latter is driven by small-scale (cm) advective processes over relatively short time scales [3,35].

There is a growing consensus that a consistent and clear delineation of "groundwater" flow paths and fluxes is needed in order to constrain coastal water and chemical budgets. The separation of water exchange pathways is particularly important in salt marshes, where differences in flow paths drive significant differences in the chemical composition of the discharged water. Water exchange pathways in a salt marsh ecosystem can be idealized from a simplified water balance (Figure 1). Within a tidal salt marsh, freshwater can recharge the sediments vertically via precipitation [31] or recharge from underlying aquifers [36]. Recharge can also occur laterally from upland, terrestrial groundwater inflow or streams connected to upland drainage basins [37]. In contrast, seawater generally recharges the sediments vertically when sea level exceeds the elevation of the marsh platform, and lateral recharge through the creek banks can occur during rising tides [17,31,32]. Water loss occurs through evapotranspiration, drawing water from the shallow sediment root zone, or by vertical and horizontal advection [16,32,33].

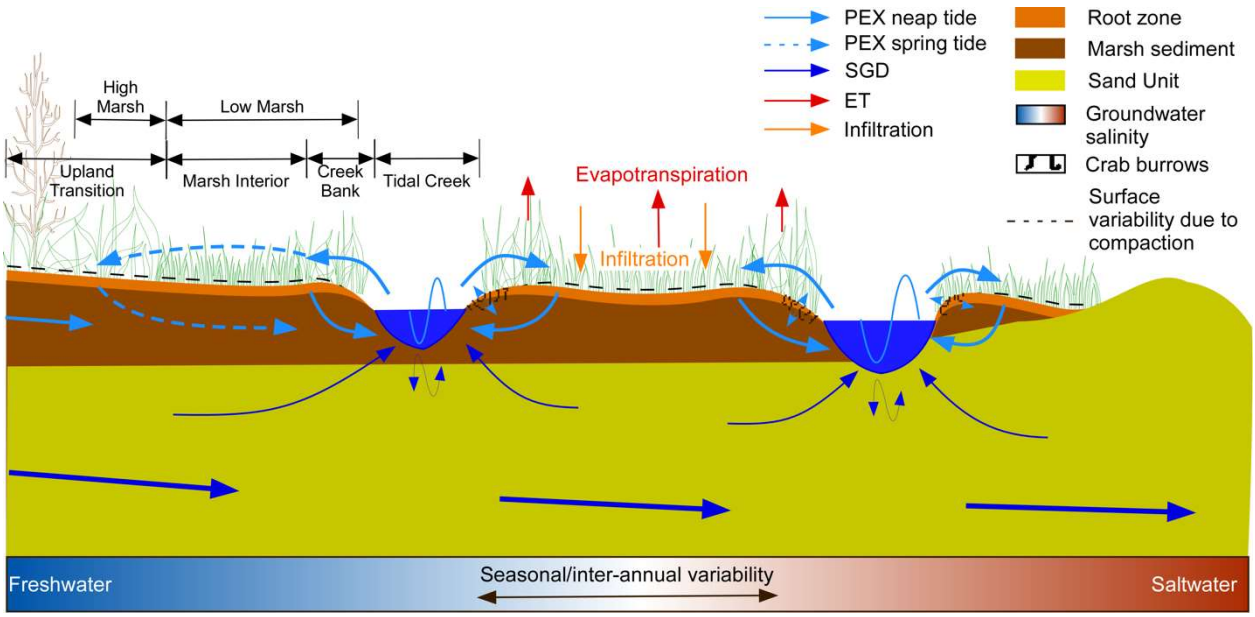

Figure 1. Conceptual diagram of a salt marsh ecosystem from the upland transition to beach environments. Color bar indicates a generalized groundwater salinity gradient across the underlying sand unit. Colored arrows show flow paths of hydrologic components (e.g., PEX, SGD, ET). Sine wave in surface water indicates tidal fluctuations in channels.

In this review, we refer to SGD when discussing water originating from an underlying coastal aquifer. SGD can be further separated into terrestrial (i.e., fresh) and marine (i.e., saline, recirculated) contributions. The former is driven by local hydraulic gradients and constitutes a new source of water (and solutes); the latter is driven by marine forcing mechanisms, including density-driven flow. In contrast, marsh porewater drainage (hereafter marsh porewater exchange or PEX for simplicity) is used to refer to water exclusively within the overlying sediments of the marsh platform and can be further separated based on marine driving forces and key depth zones. For example, Tamborski et al. [6] separated PEX from a marsh platform as interfacial (near-surface) and deep (lateral) flow paths, driven by tidal/wave overtopping and tidal pumping, respectively. It is important to note that within this conceptual framework, marsh PEX is not bound by the spatial and temporal scales defined by Taniguchi et al. [3], and thus we acknowledge that porewater drainage is a subset of SGD. However, given this review's focus on highlighting the connection between salt marsh hydrogeology and coastal chemical budgets, porewater drainage or PEX is used to differentiate water from aquifer and marsh units, consistent with the mangrove hydrogeology community [38–41].

On the surface of the marsh, there has also been a lack of consistency in reference to location on the marsh platform. Marsh platforms are delineated based on elevation, vegetation, hydrology or eco-hydrology depending on the discipline of interest. These inconsistencies are due to the fact that one terminology does not satisfy the many unique characteristics of marsh environments across the globe. Furtheremore, because of the complex couplings of abiotic and biotic factors, these delineations do not necessarily overlap. For example, the terms 'low marsh' and 'high marsh' refer to the marsh platform elevation with respect to the tidal datum, which often aligns with abrupt vegetation shifts. However, this terminology overlooks the unique hydrology of the marsh levee [13] or upland boundary [37] and the complex soil characteristics mediating vegetation zonations such as soil saturation and salinity [12,42,43]. Moffett et al. [12] developed a delineation based on root zone characteristics termed 'ecohydrological zones', which incorporated sediment, vegetation, and topographic variability. Work by Wilson et al. [37] further supported this delineation, showing that in marshes with elevated creek–marsh–upland connectivity hydrologic patterns supported distinct vegetation zonations. Xin et al. [44] delineated

the marsh based on unique hydrologic zones, and, more recently, Guimond et al. [13] delineated the marsh based on 'hydro-redox zones' to highlight the link between hydrogeological and biogeochemical processes. This delineation isolated the near-creek zone, the marsh levee, and the interior of the marsh. For the purpose of this review and simplicity, we will use the terms 'low marsh' to reference the diurnally inundated areas often dominated by *Spartina alterniflora* and 'high marsh' to refer to areas inundated on spring tides (Figure 1). However, it is important to remember that these zonations are generalizations across marshes with distinct microtopography, biogeochemistry, and hydrology which may impact the quantity and composition of exchanged water.

3. Drivers of SGD and PEX in Salt Marsh Ecosystems

There are a multitude of mechanisms driving groundwater–surface water exchange in tidal marshes that act dynamically across multiple spatial and temporal scales. Drivers are delineated by hydrogeological distinction (SGD, PEX) as well as marsh zonation.

3.1. Driving Forces of SGD

In general, fresh SGD in coastal environments is driven by land–sea hydraulic gradients [45]. On long time scales (months to decades), seasonal changes in sea level and groundwater table elevation [46] impact hydraulic gradients between the upland-marsh-ocean transition and in turn the magnitude of SGD [47]. On shorter time scales (days to weeks), tidal oscillations impact the instantaneous SGD rate by changing the hydraulic gradient between the coastal ocean and unconfined aquifer. Whereas diurnal or semi-diurnal tidal oscillations play a larger role in mediating PEX (see below), longer time scale tidal oscillations (i.e., spring–neap) impact both PEX and SGD. Wilson et al. [48] showed that SGD decreased by as much as an order of magnitude during non-inundating tides (neap tides) compared to inundating tides (spring tides) due to low creek water levels during spring low tides that produced a greater hydraulic gradient. During high tidal stages, compression of marsh sediments can further enhance groundwater–surface water exchange [49].

Extreme events, including storm surges and excessive precipitation, can temporarily impact the land–sea hydraulic gradients and thus marsh SGD. Measurements of these hydrological changes and the impact on both marsh SGD and PEX are few due to the logistical challenges of field sampling during extreme events. Wilson et al. [48] measured hydraulic heads from coastal monitoring wells and found that net groundwater discharge was reduced by half during storm surges. This reduction was attributed to the high water level in the tidal channel which temporarily suppressed discharge [48].

3.2. Driving Forces of Porewater Drainage (PEX)

Porewater drainage in salt marsh sediments is predominantly driven by tidal oscillations (Figure 1) [50–52]. Like SGD, lateral (i.e., horizontal) PEX is facilitated at ebb and low tides due to an enhanced horizontal hydraulic gradient between the marsh platform and the tidal creek [50]. Porewater drainage is also impacted by soil stratigraphy and compressibility [44]. Recharge occurs during rising and high tide when seawater overtops the marsh platform and creekbanks [50,53]. Tidal signals propagate downward and laterally into marsh sediments; attenuation of the tidal signal within the marsh sediments is related to the sediment characteristics (hydraulic diffusivity) and relative distance from the tidal creek [17,33,50]. Further, numerical simulations have shown that exchange is proportional to tidal amplitude and the elevation (including slope) of the marsh platform [54]. Thus, near-creekbank and low marsh elevation zones are disproportionately impacted by tidal pumping, as compared to higher elevation, interior marsh zones (Figure 1) [6].

Waves and tides also drive shallow PEX when the marsh platform is overtopped with seawater (Figure 1). As sea level rises, the proportion of the marsh platform inundated at high tide and the hydroperiod will increase. Initially, this can enhance water exchange pathways; however, once the marsh platform becomes fully inundated, sediment flushing will likely decrease [54]. Thus, wave pumping and tidal overtopping also disproportion-

ately impact lower elevation marsh zones. Tamborski et al. [6] suggest that overtopping drives PEX in the upper five cm of a Cape Cod salt marsh, while Bollinger and Moore [55] estimated shallow (<10 cm) porewater residence times between one hour and two days in a South Carolina salt marsh. Flushing depth is further influenced by the active root layer, which partially controls the depth of the marsh water table [12].

Crab bioturbation creates macropore structures that impact the flushing depth and magnitude of water exchange in tidal marshes, as well as erosion potential [56] and evaporation [57]. Crab burrows, which are most abundant near tidal channels [13,58,59], can increase the effective permeability of the near-creek sediment by as much as an order of magnitude [13], resulting in enhanced PEX. Xiao et al. [14] used two modeling approaches (discussed further in Section 4.1.3) to represent bioturbation and showed that the presence of burrows enhanced creek bank infiltration by a factor of 8 and exfiltration by a factor of 6. Xin et al. [60] explored the impact of both burrowing and stratigraphy on marsh seepage. Results showed that burrows increased the net groundwater–surface water exchange by 3.5% or greater when the difference in permeability between sediment layers increased, suggesting that burrows act as conduits of flow to higher permeability layers [60].

The aforementioned mechanisms operate over hourly time scales that may be imprinted by longer time scale forces (Figure 1). For example, both SGD and PEX can vary by a factor of two between spring and neap tides [47]. The El Niño Southern Oscillation (ENSO) and North Atlantic Oscillation (NAO) climate modes can drive variation in mean sea level and thus the hydraulic gradient [61]. Hydrologic setting (i.e., recharge limited or topography limited) impacts how terrestrial water table gradients respond to sea level rise, impacting predicted trends of SGD [62]. Lastly, climate change driven shifts in seasons and air temperature may impact species distributions, specifically marsh crabs [63], potentially impacting PEX across a larger latitudinal range [13]. The impact of storm events on marsh PEX is unclear and requires further study.

4. Methods

SGD and PEX can be quantified across a range of scales, from local to regional scales, and from tidal to annual (Table 1). While each scale or method has its associated uncertainties and limitations, certain methodologies may be better suited for specific questions and ecosystem types, though use of multiple methods is preferable. Below we discuss the advantages and limitations of field methodologies and model techniques with respect to salt marsh ecosystems, noting that this is not an exhaustive list of methodologies used in salt marshes but rather represents some of the most commonly employed approaches in the hydrogeologic and oceanographic communities.

Table 1. Summary of methods used to quantify marsh PEX (yellow shading) and SGD (blue shading), arranged by approximate spatial and temporal scales. Several methods capture both marsh PEX and SGD (green shading).

Timescale	Local-Scale		Regional-Scale	
	Marsh PEX	**SGD**	**Marsh PEX**	**SGD**
Tidal to spring-neap	Shallow wells Sediment Ra^ Porewater Ra/Rn	Deep wells Salt balance	NA	Sediment Ra^^ Salt balance
	Seepage meters * Numerical models		Tidal Ra/Rn ** Numerical models	
Seasonal to Annual	Shallow wells	Deep wells	NA	Water budget
	Numerical models		Numerical models	

* salinity dependent; ** dependent upon Ra activity ratios and endmember concentrations; ^ two-layer transport model (overlying muddy sediments); ^^ two-layer transport model (sandy underlying sediments); NA = not available.

4.1. Hydrologic Approaches

4.1.1. Direct Measurements

Direct measurements of SGD and PEX are conducted using "manual" or Lee-type seepage meters, which, in the simplest form, includes a chamber installed in the sediment connected to a plastic bag. Seepage meters have been extensively used in freshwater [64] and marine environments, particularly sandy marine settings [65]. Seepage meter construction is inexpensive, both in time and materials [65,66]. More expensive instruments include automated or more advanced ultrasonic, heat pulse, or dye-dilution techniques [67–69]; however, these devices do not physically capture discharging fluids and have seen limited application in marsh environments. Individually, Lee-type seepage meters only capture a small area, approximately 0.26 m^2 (the area of the top of a 55-gallon steel drum). However, transects with multiple meters simultaneously sampling can be an effective method to quantify SGD and PEX and resolve spatial heterogeneity. Lee-type seepage meters provide one of the only direct measurements of SGD and PEX, and water collection enables chemical analyses and salinity measurements of the discharged water. While best practices for seepage meters in freshwater and marine environments have previously been discussed [64,65,70], the following factors should additionally be considered when conducting manual seepage meter measurements in salt marshes.

Tidal Oscillations. Tidal channels often drain to water depths on the order of centimeters in secondary and tertiary channels. Conventional seepage meters must be completely submerged for data collection [65] and thus require careful observation during falling tides to ensure that bags are removed prior to meter or outlet exposure. This is particularly relevant for narrower channels that become completely exposed at low tides. Seepage meters may be more effective in large salt marsh channels where low tide does not expose significant areas of the channel bank and bottom [71]. However, as noted by Gardner [72], measurements must be conducted along the entire channel bottom and muddy creek bank to capture the full magnitude of SGD and PEX.

Sediment Type. Channel sediment varies depending on salt marsh location and can be layered with a sandy channel bottom overtopped by mud or completely encased in mud from channel bank to bottom (Figures 1 and 2). Sandy channels may enable successful seepage meter measurements due to more homogenous bottom sediments, generally higher flux rates (i.e., higher K), and low risk for sustained sediment disturbance. In contrast, mud to clay encased channels make seepage meters difficult to deploy. Pushing meters into the muddy substrate is initially easy, but disturbances near seepage meters can cause excessive water flux into seepage meters, buried roots can inhibit complete enclosure of the meter, and settling of the meter into the sediment can diminish and eventually eliminate headspace. Meters should be deployed from a ladder or by swimming in order to avoid disturbing the surrounding sediment (Figure 2). Care must also be taken to seal the mud surrounding the meter, while maintaining headspace. Meters should be installed prior to sampling campaigns to ensure sediment equilibration and flushing of the meter headspace [70]. The adequate equilibration period varies due to sediment type, water flux rate, and installation depth (i.e., head space); salt marshes may require a longer equilibration time than sandy coastal environments due to their fine-grained sediments and potentially low water fluxes. It is important to note that seepage meter use is optimal when water fluxes exceed approximately 20 L m^2 d^{-1} [73,74], and along muddy marsh shorelines, SGD fluxes can be much lower.

Seepage Meter Case Study. These challenges are known in part from experience, yet despite these considerations, seepage meter measurements can provide important insight into SGD and PEX in salt marshes. To show the importance of direct discharge measurements, the following section will discuss a seepage meter study in a Delaware tidal marsh. Two seepage meter surveys were conducted over a single tidal cycle on 26 August 2016 and 2–3 March 2017 in a tidal channel at St. Jones National Estuarine Research Reserve in Dover, Delaware. Seepage meter construction and deployment were similar to as described by Russoniello and Michael [75]. Sixteen seepage meters were

deployed during each campaign and arranged in two rows perpendicular to the tidal channel, covering the banks and bottom of the channel (Figure 2). Meters were installed one day prior to sample campaigns. Plastic bags affixed to a quick attach/release fitting were prefilled with 2 L of water to enable quantification of water fluxes into and out of the sediment. The average time of deployment was 75 min. Bags were promptly weighed after deployment. As discussed above, due to tidal oscillations in the creek, not all seepage meters could be measured each sampling period. If any part of the seepage meter was above the water level, measurements were discontinued. To minimize disruption of the sediment near seepage meters, ladders were deployed across and along the channel for bag deployment and collection (Figure 2).

Figure 2. Example photographs of seepage meter campaigns in a Delaware salt marsh. Photos show (**a**) and (**b**) seepage meters installed in a creek bank and channel bottom with a ladder across the marsh; (**c**) a closer look at the ladder across the creek and a second ladder for access to the seepage meters; and (**d**) a perpendicular view of the ladder set-up and additional piezometer instillation.

Measurements showed spatial and temporal variability in the magnitude and direction of water exchange between the marsh platform and tidal channel (Figure 3). In general, the exchange rates from individual seepage meters ranged from −10.8 to 9.5 cm d^{-1} in August and from −9.7 to 7.0 cm d^{-1} in March. Negative exchange rates indicate recharge into the marsh platform and positive exchange rates indicate discharge into the channel. The average net exchange rate in August was 0.4 cm d^{-1} and ranged between 0.1 and −0.1 cm d^{-1} on the first and second sample day in March, respectively. The average discharge in August was 2.2 and 1.3 cm d^{-1} in March. This disparity is in part due to the difference in tidal range between August and March sample dates (~0.8 masl and ~0.5 masl in August and March, respectively).

Spatially, the flux rate varied between the channel bank and bottom (Figure 3), as well as between individual seepage meters on the bank or bottom. Average discharge was greater from the channel bottom compared to the channel bank. In August, the average discharge from the bank was 1.7 cm d^{-1}, and the average discharge from the bottom was 2.3 cm d^{-1}. These findings are in contrast with work by Gardner [72] which suggests that two-thirds of discharge occurs through creek banks.

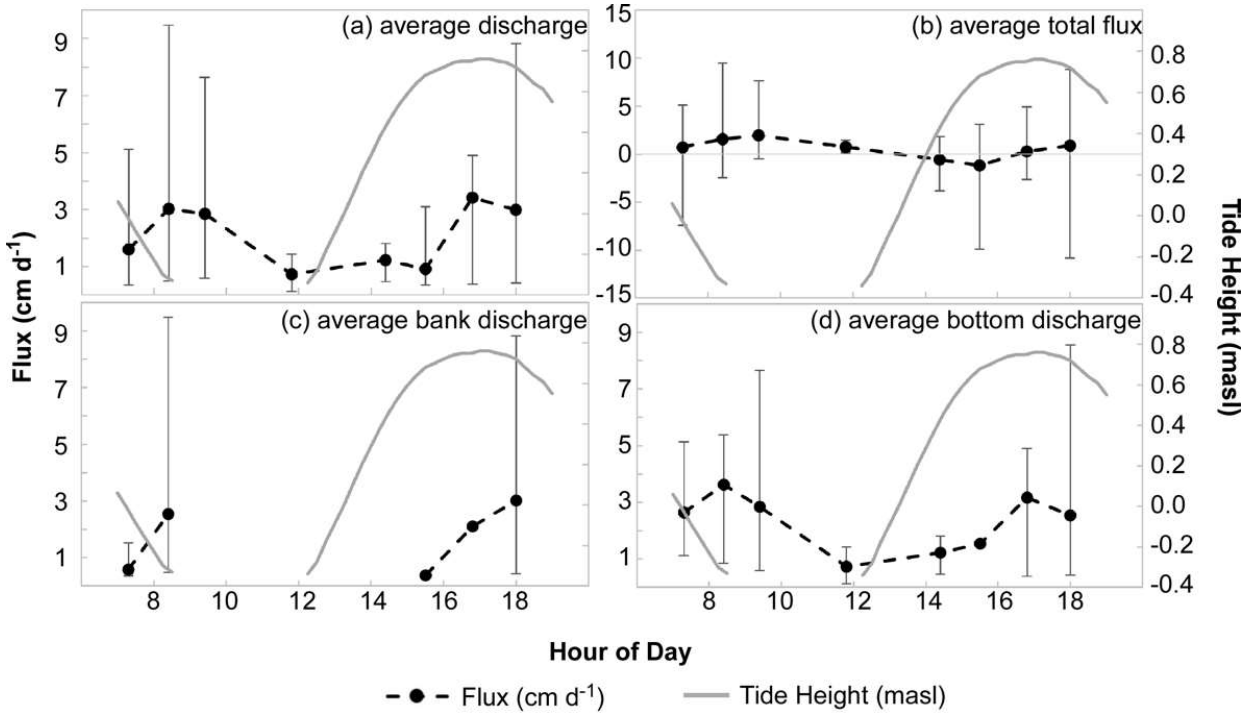

Figure 3. Seepage meter measurements from the St. Jones National Estuarine Research Reserve over one tidal cycle during an August 2016 field campaign. Measurements show (**a**) average (± measured range) discharge for all seepage meters (i.e., bank and bottom; n = 16); (**b**) average net exchange for all seepage meters (discharge + recharge); (**c**) average discharge from seepage meters in the creek bank; and (**d**) average discharge from seepage meters in the creek bottom. Note the gaps in (**c**) reflect time periods in which the seepage meters were exposed, and gaps in tide height indicate that the logger was out of water. Water level data from the Delaware Department of Natural Resources and Control.

Within the same sample period, exchange measurements varied in magnitude and direction by as much as 19.6 cm d^{-1} in the bank and 8.2 cm d^{-1} in the creek bottom. For example, within the same time frame, seepage meters located side-by-side along the creek bank had measured exchange rates of −2.5, 1.2 and 9.5 cm d^{-1}. Meters aligned in the creek bottom varied from −0.4 to 5.1 cm d^{-1}. This localized variability may be attributed to preferential flow paths created by roots and crab burrows. During both August and March field campaigns, *Spartina* root clusters were visible in the bank and bottom of the channel. While these hollow stems may conduct air and oxygen into the otherwise anoxic sediment, they may also conduct water between the tidal channel and marsh platform. Additionally, in August, crab burrows were visible in the creek bank and on the near-creek marsh platform [13].

Temporally, both the net exchange rate and discharge rate were greatest during ebb tide when the hydraulic gradient between the marsh platform and creek was greatest. The net exchange rate and discharge rate were lowest during rising tide when water was recharging the creek bank (Figure 3). These findings are similar to those of Xin et al. [17], who suggested that creek water recharges the marsh platform on rising tides, creating a near-creek swash zone rather than a previously conceptualized near-creek circulation cell (e.g., Figure 1). The insight gleaned from this case study highlights an important benefit of direct measurements: the ability to capture small-scale variability in exchange due to environmental heterogeneity. Thus, we suggest conducting direct seepage measurements in combination with less labor-intensive indirect measurements discussed below.

4.1.2. Indirect Approaches

Groundwater–surface water exchange can be inferred from piezometers and water level measurements by determining hydraulic gradients. Vertical hydraulic gradients from

piezometer nests in channel bottoms or lateral hydraulic gradients between the marsh platform and creek can be used with estimates of hydraulic conductivity (K) to estimate exchange via Darcy's Law (Equaiton (1))

$$Q = -KA\frac{dh}{dL} \quad (1)$$

where Q is the volumetric water flux ($m^3\ d^{-1}$), K is the hydraulic conductivity ($m\ d^{-1}$), dh/dL is the hydraulic gradient and A is the cross-sectional area of the seepage face (m^2).

Anisotropic and heterogeneous marsh sediments inherently produce uncertainties in estimating a representative hydraulic conductivity for flux calculations. Hydraulic conductivity (K) can be estimated from bail or slug tests [76], infiltration rings [77], pedotransfer functions [78], permeameters [79,80], or by determining sediment diffusivity and average specific storage [47,81]. Further uncertainty is introduced in estimating the area of the discharge zone; however, Darcy-based approaches can reasonably track temporal variability in discharge over time in marsh environments [47]. Similar to seepage meters, nested piezometers reflect a single point in space, and care should therefore be taken to install multiple wells over a representative area. Gardner [82] notes that special care must be taken for well installation in tidal wetlands, where piezometer screens may be easily clogged, and summarizes recommendations for choosing an appropriate well diameter and screen length for different marsh sediment and environmental (i.e., tidal range) characteristics.

Water table elevation monitoring (in wells) and its response to precipitation can also be used to infer porewater exchange by estimating an "effective" specific yield [83]. If rainfall (mm) is positively correlated with well water level response (mm), then the slope of this regression can be divided by the mean drawdown ($m\ tide^{-1}$) and representative transect width (m) to estimate porewater drainage ($m^3\ tide^{-1}$). This method is unable to capture porewater drainage in regularly flooded marshes with shallow water tables, and care must be taken to ensure that wells are properly designed to capture the unique response dynamics of low hydraulic conductivity marsh soils [82].

Terrestrial groundwater discharge can be simply constrained from a salt balance and measurement of water flow through a tidal channel over time [20]. Salt balances can also be written to describe the effects of advection and dispersion in marsh pore waters [34]. Under steady-state conditions (one dimensional), the distribution of salt will be balanced by vertical upward groundwater advection and vertical downward diffusion of salt. In addition, terrestrial groundwater discharge can be approximated from a water balance, which assumes a net-zero tidal flow, losses via evapotranspiration (ET) and gains via terrestrial groundwater [34,84] (Figure 1). However, estimations of ET can be difficult to constrain [85].

4.1.3. Numerical Models

Numerical models have been extensively used to simulate near-creek hydrogeology and tidal creek-marsh platform interactions [17,50,72]. Early studies on the flux of water between marsh platforms and tidal channels used boundary integral equation method (BIEM) models, which can simulate isotropic, homogeneous, and saturated vertical and horizontal flow with seepage face dynamics [72,86]. Gardner [86] used a BIEM model to assess the impact of marsh channel geometry on seepage magnitude and location and a similar model was used by Gardner [72] to assess spatial and temporal dynamics of porewater seepage. As argued by Gardner [86], simplistic models enable a clear assessment of links between observed properties and characteristics that are not obfuscated by parameters and site-specific characteristics.

These pioneering studies were essential to our foundational understanding of marsh-creek PEX and highlight the need for more complex modeling studies. For example, Gardner [72] showed that approximately 80% of (seawater) recharge occurs within 3 m of the tidal channel, and thus a majority of seepage is hypothesized to occur within a near-creek circulation cell (Figure 1). This knowledge in combination with our understanding of

the impact of channel geometry on seepage suggests that three-dimensional models that incorporate microtopography, evapotranspiration and precipitation are important for quantifying ecosystem-scale PEX. Additionally, the important role of hydrogeologic parameters (e.g., K, Sy) on seepage magnitude [50] highlights the importance of heterogeneous and anisotropic models that can capture marsh stratigraphy and bioturbation.

Finite element models such as SUTRA, HydroGeoSphere and FlexPDE can be used to simulate more complex marsh-creek domains that consider sediment heterogeneity [14,50,60], solute dynamics [87,88], and coupled surface–subsurface water flow [62,89]. With added computational and domain complexity, new considerations need to be addressed. Formulation of aquifer compressibility and total stress impacts salt marsh seepage and groundwater flow [90]. Tidal inundation increases the total stress on the submerged portion of the marsh platform and thus the assumption of standard groundwater flow models, that total stress is constant, no longer holds [91]. The governing equations for various representations of compressibility and total stress are discussed in Gardner and Wilson [90]. However, numerical tests by Xin et al. [60] suggest that the effects of compressibility on porewater flow are negligible when hydraulic conductivity is greater than 10^{-6} m s^{-1} and thus neglected compressibility terms altogether. Given the potential relevancy to quantifications of SGD and PEX, it is recommended studies incorporate sensitivity analyses that explore the impact of including or excluding compressibility in the governing flow equation.

Heterogeneity due to macropores such as crab burrows or roots is an important consideration and can be modeled via two methods: (1) preferential flow model and (2) equivalent-continuum model [14]. In preferential flow models, burrows are explicitly modeled as zones of high *K* in contrast to the lower *K* matrix (i.e., dual porosity and dual permeability); equivalent-continuum models incorporate bulk properties of the bioturbated matrix. Xiao et al. [14] compared both methods to assess the utility in simulating water and solute fluxes in marsh-creek systems and found that preferential flow models are more realistic, particularly when simulating solute fluxes. Yet preferential flow models require finer mesh resolution, at least in bioturbated areas, and thus can be more computationally intensive than equivalent-continuum models which are simpler and allow coarser mesh while still capturing bulk flow properties.

The incorporation of variable salinity and density-driven flow also influences SGD and PEX [88,92]. In some cases, salinity and density-driven flow may be overlooked when salinity contrasts and variations across field sites are small [60,62]. Due to the added computational complexity, incorporation of variable density and density-dependent flow will depend on the question and study site and should be incorporated into a sensitivity assessment. Similarly, evapotranspiration is an important, yet complex, component of salt marsh water and salt budgets. Modeling approaches for salt marsh evapotranspiration are described in Moffett et al. [93] and Moffett and Gorelick [94].

Lastly, assigned boundary conditions impact simulated salt marsh hydrogeology. Most two-dimensional marsh groundwater models are formulated as in Figure 4a. However, recent studies have highlighted the importance of upland water tables in governing salt marsh hydrogeology and SGD [37,62], and thus more complex upland conditions that reflect the local groundwater table elevation landward of the marsh may need to be incorporated (Figure 4c). Similarly, deeper models that extend below the marsh sediments and can capture the terrestrial inflow or saline recirculation may also need to be incorporated in order to capture all drivers of PEX and SGD.

4.2. Geochemical Approaches

Naturally occurring radium isotopes and radon are often highly enriched in coastal groundwater over surface waters, making them effective tracers of groundwater–surface water exchange [95]. These radioisotopes are produced by the decay of their U/Th series parents in geological matrices and generally behave conservatively once they enter the marine environment, as they are not readily taken up by biological processes [96]. Their unique half-lives (^{222}Rn = 3.8 d; ^{223}Ra = 11.4 d; ^{224}Ra = 3.6 d; ^{226}Ra = 1600 y; ^{228}Ra = 5.75 y)

enable tracing different processes and flow paths occurring over time scales of hours to decades. One key difference over other methods is that radionuclides are integrative tracers that tend to smooth out small-scale heterogeneities that plague other measurement techniques (e.g., seepage meters).

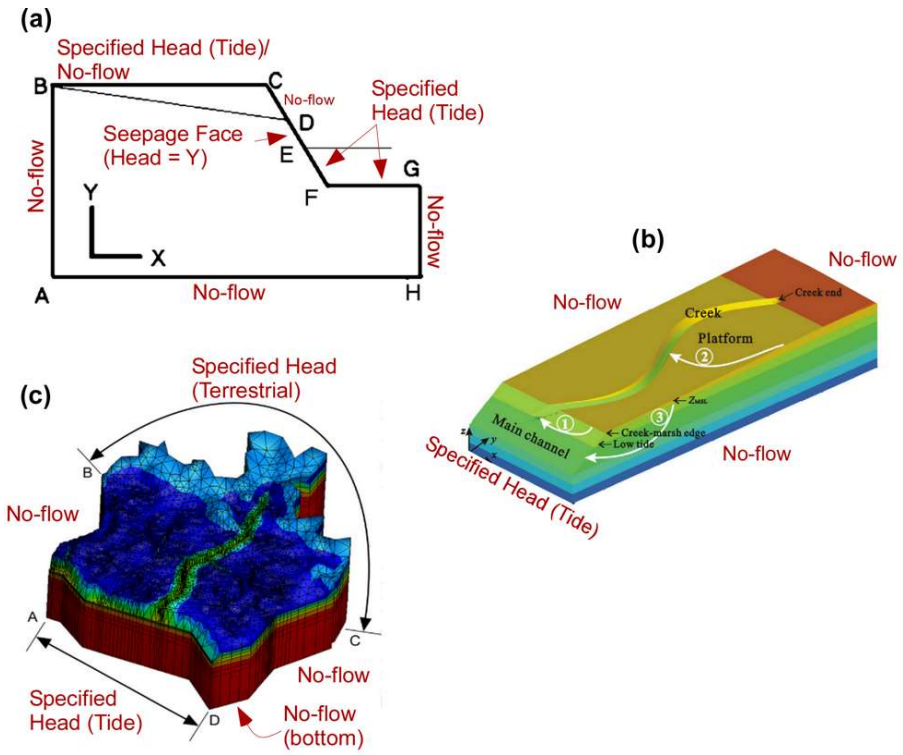

Figure 4. Examples of two- and three-dimensional model domains. Figures were modified from Gardner [72,86], Xin et al. [17], and Guimond et al. [62] for (**a**–**c**), respectively.

Utility of dissolved Ra isotopes as tracers of groundwater–surface water exchange in salt marshes was first documented by Bollinger and Moore [97]. In this seminal study, the authors observed clear increases in ^{224}Ra and ^{228}Ra activities in a tidal creek (North Inlet, SC, USA) with decreasing tidal water levels, and over multiple seasons [55]. Rama and Moore [98] later concluded that such changes in tidal creek Ra activity must be driven by groundwater discharge. Below, we highlight different Rn- and Ra-based techniques to quantify groundwater–surface water exchange over different spatiotemporal scales in salt marsh ecosystems.

Porewaters. Rama and Moore [98] developed a steady-state, one-dimensional box model to describe the distribution of Ra in salt marsh sediments and porewaters considering exchange between a deep layer (sandy aquifer), surface layer (fine-grained deposits) and tidal creeks. Subsequent one-dimensional reactive-transport models have been developed considering advection, production, decay and adsorption/desorption reactions to describe measured porewater Ra activities [99,100],

$$A(x) = \frac{P}{R} + \left(A_o - \frac{P}{R}\right) e^{-\Delta x \lambda R v^{-1}} \quad (2)$$

where A_x is the Rn or Ra activity (Bq m^{-3}) at distance x, A_o is the initial Rn or Ra activity (e.g., tidal creek water), P is the radionuclide production rate (Bq m^{-3}), λ is the radionuclide decay constant (d^{-1}), R is the linear retardation factor for Ra transport (dimensionless; radium only) and v (m d^{-1}) is the advective velocity; note that dispersion is assumed negligible with respect to advection in Equation (2). Successful application of the above model requires the following conditions: steady state, a constant sediment production

rate with depth (P), a constant solid–solution partitioning (R), and that surface waters are deficient in the modeled Rn or Ra isotope compared to porewaters.Conditions related to a constant P and R may not be met in salt marsh ecosystems where fine-grained deposits overlie sandy sediments. The one-dimensional reactive-transport model is best suited for shallow (<1 m) one-dimensional flow systems with constant porewater salinities such as freshwater wetlands [99] and island (saline) marshes [101] and may not be suitable in fringing marshes influenced by terrestrial groundwater flow. We also note that porewater collection can be difficult in muddy marsh environments when fine-grained sediments clog the piezometer screen. Care should be taken to filter out suspended particles (typically enriched in parent Th isotopes) in porewater and estuarine water samples for dissolved radium measurements.

Sediments. Measurement of ^{224}Ra:^{228}Th disequilibrium in marsh sediments overcomes the requirement of a constant production rate in the above porewater-based model [102]. Analysis of ^{224}Ra and its particle-reactive parent ^{228}Th ($t_{1/2}$ = 1.9 y) can reveal the depth and relative magnitude of marsh sediment flushing over a time scale of approximately ten days. Under steady-state conditions the activity of ^{224}Ra should equal its parent ^{228}Th (^{224}Ra:^{228}Th activity ratio = 1). Transport of the more soluble ^{224}Ra daughter from porewater into overlying waters may be produced by some combination of molecular diffusion, bioirrigation and bioturbation, and physical advective processes, resulting in activity ratios less than one. Sediment deficits of ^{224}Ra with respect to ^{228}Th can be integrated to derive a ^{224}Ra flux, which in turn can be used to calculate both rates of water exchange and solute transport [103]. This approach has been successfully applied to estimate the benthic flux of methylmercury [104] and the advective transport of oxygen [105] from intertidal muddy marsh sediments. Shi et al. [103] developed a two-layer transport model to describe water and solute (P, Mn, Fe) transport between mud and sand layers from a marsh in North Inlet, SC, where marsh PEX and SGD carry substantially different solute loads. Using the two-layer transport model in a microsalt marsh (Sage Lot Pond, MA, USA), Tamborski et al. [6] revealed that near-surface sediment flushing (0–5 cm depth) was driven by wave and tidal overtopping, while the majority of PEX (and DIC export) occurred at the subsurface sediment horizon intersected by mean low tide, driven by tidal pumping. In marsh systems, sediment cores should be taken sufficiently deep with adequate vertical resolution in order to qualitatively resolve key depth horizons of sediment flushing. Further, marsh sediment cores should be carefully collected to minimize sediment compaction, as for example, with a Russian Peat Borer.

Surface Waters. Mass balances are commonly utilized to estimate groundwater–surface water exchange in marsh tidal channels [26,106,107] and semi-enclosed estuaries [108]. By accounting for all the known sources (e.g., rivers, sediments) and sinks (e.g., radioactive decay, mixing losses) of a particular Rn or Ra isotope in a given system, the tracer flux driven by SGD and/or PEX can be estimated (SGD or PEX = $\sum$ tracer sinks $-$ $\sum$ tracer sources). Dividing this tracer flux (Bq d^{-1}) by the representative groundwater or porewater activity (Bq m^{-3}) thus yields a rate of water exchange (m^3 d^{-1}). In layered marsh systems, the rate of seawater circulation through the sediments and the rate of Ra production between the different sediment layers will lead to unique endmember Ra activity ratios [109]. Thus, multiple endmember mixing models can be developed to discriminate between terrestrial SGD and marsh PEX (e.g., Figure 5). This approach can be applied at a stationary time-series location or over a larger area at a single point in time (e.g., Charette and Buesseler, [110]).

Organic-rich salt marsh sediments often have a relatively low ^{226}Ra sediment pool available to produce dissolved ^{222}Rn, and thus salt marsh porewaters are generally low in ^{222}Rn compared to sandy beach environments. When ^{222}Rn is depleted in marsh porewater, its measurement in tidal creek and estuarine waters may be useful in isolating terrestrial SGD. In mineral-rich marsh environments, ^{222}Rn may be an effective tracer of groundwater–surface water interactions [39,49] and is a particularly effective tracer in mangrove wetlands [38,111].

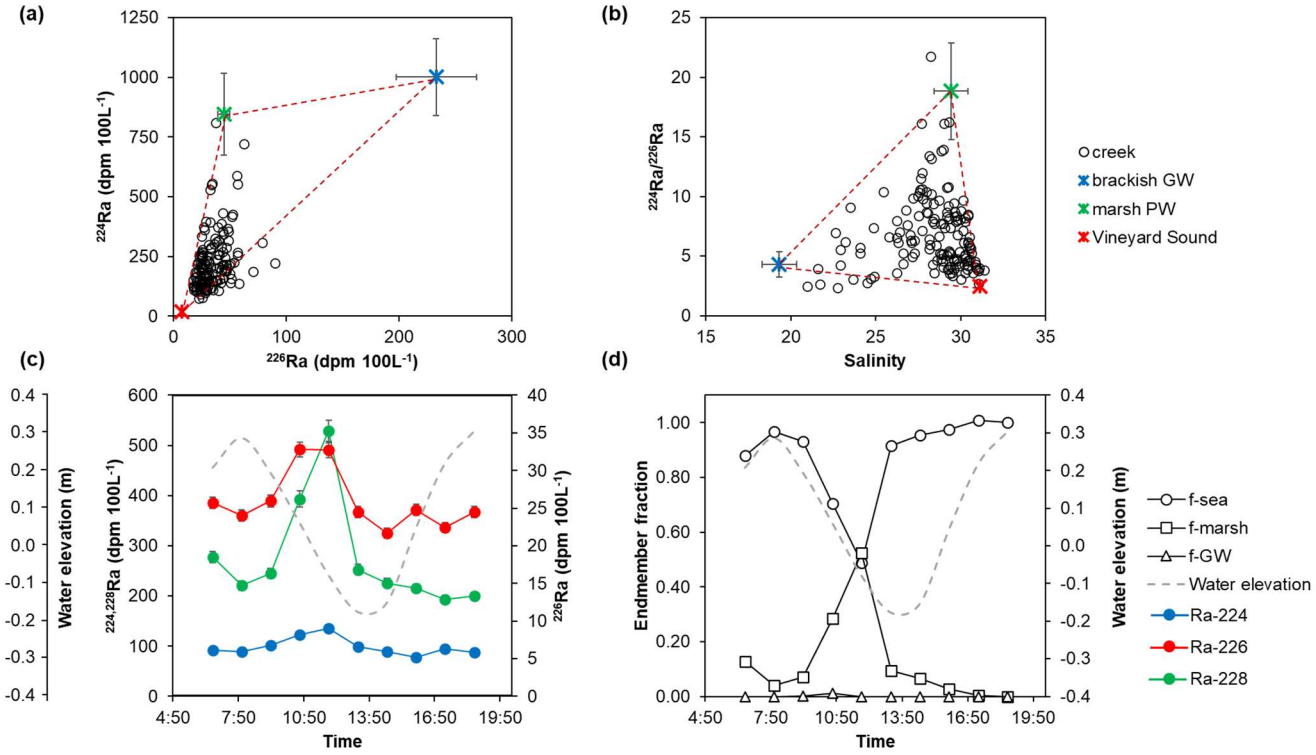

Figure 5. Tidal creek, porewater and groundwater radium isotopes from a microtidal salt marsh (Sage Lot Pond, MA, USA), adapted after Tamborski et al. [6]. Variation in ^{224}Ra versus ^{226}Ra (**a**) and ^{224}Ra/^{226}Ra activity ratios versus salinity (**b**). Hourly variation in Ra activity and creek water elevation during a tidal cycle (**c**) with results of the ^{224}Ra/^{226}Ra endmember mixing model (**d**). The unique ^{224}Ra/^{226}Ra ratio of seawater (Vineyard Sound), marsh porewater and brackish groundwaters was used to discriminate between these different pathways to derive endmember fractions of marsh PEX (f-marsh; squares) and brackish SGD (f-GW; triangles).

5. Literature Synthesis

All measurements of SGD or PEX provide important insight into spatial and temporal trends, regardless of the methodology. To this end, information on tidal range, PEX and SGD rates were compiled from 33 studies for 19 different locations. Studies were only considered that calculated area-normalized rates or considered whether the total flux could be easily converted to an area-normalized rate based on available information. These studies span spatial scales from meters to several kilometers, and time scales from tidal to annual. An average PEX and SGD rate was estimated for each study site if seasonal data were available, and additionally when there were multiple studies for the same location, regardless of the methods used.

5.1. Results

All the compiled studies were located on the US East Coast, except for two studies in Australia and one in China (Figure 6; Table 2; Table S1). Approximately 82% of the studies were in microtidal environments (<2 m) and there were no studies located in macro or megatidal environments (>4 m). This geographical bias focused on US East Coast microtidal settings precludes representative upscaling, as needed, for example, in regional (coastal) carbon budgets [5]. Further, only six of the 19 study sites captured seasonal and annual variations in groundwater–surface water exchange. Field and numerical modeling studies have been conducted in other locations, including the US West Coast [12], Bay of Fundy, Canada [77] and China [88,112]; however, area-normalized flux information is unavailable and therefore these locations are not discussed here.

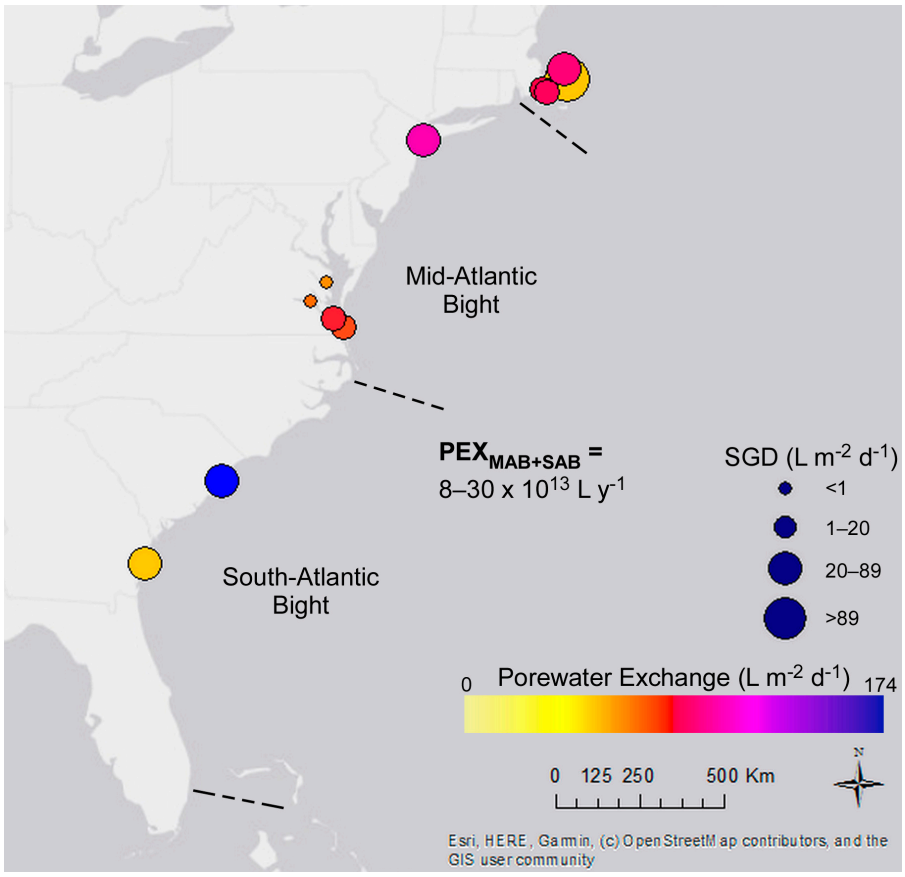

Figure 6. Map of the East Coast of the Unites States showing compiled salt marsh field sites with average PEX depicted by color and the average SGD rate depicted by symbol size. Dashed lines approximately delineate the Mid-Atlantic and South Atlantic Bights.

Table 2. Summary of average area-normalized marsh porewater and groundwater flux estimates, derived from Table S1. Groundwater includes brackish and freshwater fluxes. Note that tidal range for each site is an approximation. n/a indicates "not available".

Location	Tidal Range (m)	Pore Water Flux	Groundwater Flux	References
		L m^{-2} d^{-1}	L m^{-2} d^{-1}	
Belle Isle, MA, USA	2	3	n/a	[33]
Nauset Marsh Estuary, MA, USA	1.3	n/a	48	[113]
Great Sippewissett Marsh, MA, USA	1	18	8	[18,20,106,114–116]
Pamet River Estuary, MA, USA	3	47	67	[109]
Sage Lot Pond, MA, USA	0.5	40	20	[4,6]
Jamaica Bay, NY, USA	1.5	99	89	[101,108]
St. Jones NERR, DE, USA	1.2	22	n/a	this study
Carter Creek, VA, USA	0.8	9.2	1	[34]
Eagle Bottom, VA, USA	0.8	10.3	0.2	[34]
South Hog Island, VA, USA	1.4	120	n/a	[117]
Ringfield Marsh, VA, USA	1	11	7	[84]
Elizabeth River Estuary, VA, USA	1	12	11	[110]
North Inlet, SC, USA	1.4	174	51	[26,55,71,98,103,118,119]
Folly Beach, SC, USA	1.5	54	n/a	[105]
Pritchards Island, SC, USA	2.5	115	n/a	[117]
Sapelo Island, GA, USA	2.5	n/a	63	[49,107]
Evans Head, Australia	1	106	n/a	[39]
Barwons Head, Australia	1	n/a	37	[120]
Jiaozhou Bay, China	2.7	0.03	n/a	[121]

Despite the biases noted above, some conclusions were drawn from this meta-analysis. Nine field locations (comprising 67% of the studies) have differentiated between SGD and PEX. Comparison between average rates of SGD and PEX reveals an approximately linear relationship (p = 0.038, n = 9; Figure 7). Of these nine locations, six span seasonal and annual time scales (Great Sippewisset, MA, USA; Pamet River Estuary, MA, USA; Sage Lot Pond, MA, USA; Jamaica Bay, NY, USA, Ringfield Marsh, VA, USA and North Inlet, SC, USA), all of which except Ringfield Marsh were derived from radium isotope mass balances; North Inlet was studied using multiple methods.

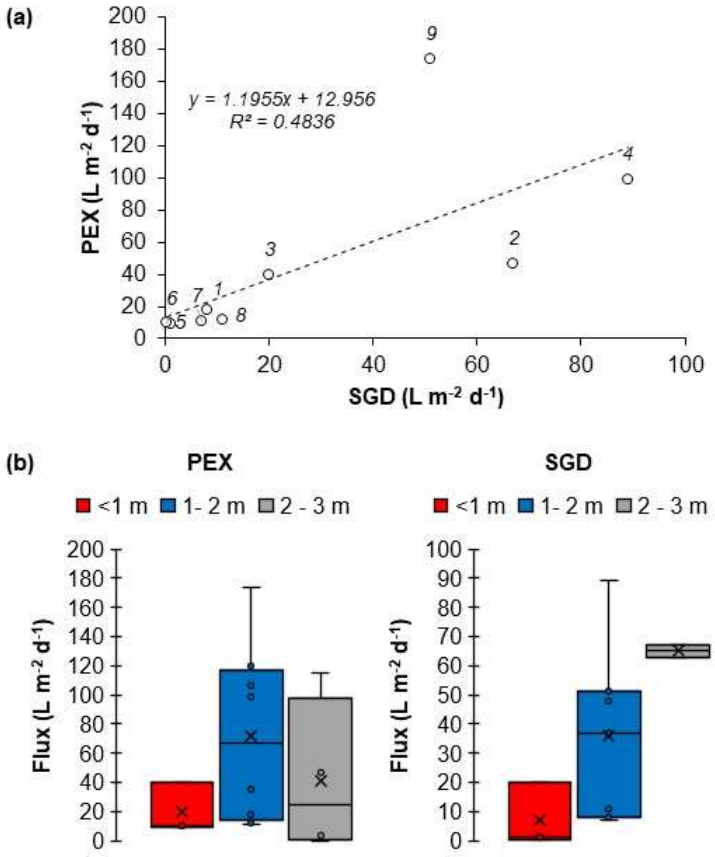

Figure 7. Comparison between mean PEX and SGD from the literature analysis (**a**). Generalized tidal range classification for all sites versus PEX and SGD (**b**). Italicized numbers in (**a**) correspond to the following sites: 1 = Great Sippewissett, MA; 2 = Pamet River Estuary, MA; 3 = Sage Lot Pond, MA; 4 = Jamaica Bay, NY; 5 = Carter Creek, VA; 6 = Eagle Bottom, VA; 7 = Ringfield Marsh, VA; 8 = Elizabeth River Estuary, VA; 9 = North Inlet, SC.

Average SGD is positively correlated with tidal range (p = 0.010, n = 12; Figure 7). This is consistent with previous work by Wilson et al. [47], where the rate of SGD from a confined aquifer beneath marsh deposits increased in magnitude with increasing tidal amplitude and decreasing mean sea level. In contrast, average PEX does not show any statistically significant relationship with tidal range (Figure 7) and thus demonstrates that the drivers of marsh PEX are multidimensional (Figure 1), as previously suggested for mangrove wetlands [38]. Tidal amplitude and thus tidal pumping alone cannot explain the complex relationship between marsh elevation, sediment characteristics, stratigraphy, bioturbation and vegetation in controlling PEX, particularly if PEX is further separated into shallow and deep flow paths [6].

SGD has been extensively studied at two marsh sites using a variety of methods: North Inlet, SC, USA and Great Sippewissett, MA, USA. Groundwater discharge to North Inlet marsh varies from 8 to 200 L m^{-2} d^{-1} (Table S1). Spatiotemporal variations notwith-

standing, radium isotope-based estimates (38–200 L m^{-2} d^{-1}) [55,98,103] are comparable but higher than estimates derived from seepage meters (8–28 L m^{-2} d^{-1}; [71]) and salt balances (10 L m^{-2} d^{-1}; [118]). In comparison, groundwater discharge to Great Sippewissett marsh varies from 1 to 26 L m^{-2} d^{-1}, with general agreement between Darcy's law (1–26 L m^{-2} d^{-1}; [114–116]), seepage meter (18 L m^{-2} d^{-1}; [18]), salt balance (14 ± 2 L m^{-2} d^{-1}; [20]) and radium isotope-based techniques (4 ± 10 L m^{-2} d^{-1}; [106]). It is important to note that these different studies were conducted over the course of several years and not necessarily the same time period or location; further, uncertainties (or lack thereof) were treated differently between studies (e.g., Howes and Goehringer [18]; Charette et al. [106]). Tobias et al. [84] found that salt balances were most accurate in quantifying groundwater discharge during times of high flux in fringing marshes while Darcy-based measurements were more robust during low discharge periods. Because each of these methods integrate over unique spatiotemporal scales, direct comparisons may not always be appropriate and should be made cautiously.

5.2. Regional and Global Significance

Tidal marshes are implicitly considered in US East Coast fresh SGD models [122]; however, regional estimates of marsh SGD and PEX are lacking. Given the number of marsh studies from the US East Coast (Table 2; Figure 6), we will attempt to upscale local estimates of PEX to a regional scale. The statistically significant relationship between SGD and tidal range (Section 5.1) prevents representative upscaling without classifying and weighting regional marsh areas by tidal regime. Average (±std) PEX along the US East Coast is 52 ± 52 L m^{-2} d^{-1} (n = 14 sites; Table 2). Considering sites that integrate over tidal, seasonal and annual time scales, PEX is between 24 and 86 L m^{-2} d^{-1}, covering the first and third quartiles of the US East Coast dataset. The area of salt marshes along the East Coast of North America is 10.13 ± 1.20 × 10^3 km^2, or 9.62 ± 1.17 × 10^3 km^2 for the Mid-Atlantic Bight and South Atlantic Bight [5,123]. Considering the Mid-Atlantic Bight and South Atlantic Bight salt marsh area, a back-of-the-envelope calculation reveals that marsh PEX is between 8 and 30 × 10^{13} L y^{-1}. As a first-order approximation, PEX may recirculate 1–4% of the Mid-Atlantic Bight and South Atlantic Bight continental shelf waters each year, considering a shelf volume of 7.70 × 10^3 km^3 [124]. In other words, it would only take ~30–90 years to recirculate the entire volume of seawater overlying the Mid-Atlantic Bight and South Atlantic Bight continental shelf through salt marsh sediments; this time scale is comparable to estimates of PEX in mangrove wetlands globally [38]. While this is a simplified estimation, it highlights the ability of salt marshes to recirculate significant volumes of seawater and clearly demonstrates the importance of salt marsh hydrogeology on coastal ecosystems at local and regional scales.

Tidal wetlands export 4.2 ± 1.3 Tg of total carbon per year to estuaries and shelf waters along the Eastern North America coast, with approximately equal contributions from dissolved inorganic and organic carbon species [5]. If the range in regional PEX above is reasonable, then what would be the regional marsh porewater carbon concentration (endmember) necessary to sustain this annual export? Considering the first and third quartiles of the US East Coast dataset, regional marsh porewaters would be enriched in DIC or DOC over seawater (i.e., net-zero water flux but net solute flux) between 0.5 and 1.8 mM C. Enrichment of porewater DIC over seawater concentrations (~2 mM C) is broadly related to aerobic and anaerobic respiration (i.e., sulfate reduction) within salt marsh sediments and this range of values is conservative, as compared to field observations (i.e., [6,39,125]). The inorganic nitrogen endmember produced via internal marsh sediment respiration would be between 70 and 260 μM N for US East Coast marshes (assuming a Redfield ratio of 106 C: 16 N), or N mineralization rates of ~10–110 g N m^{-2} y^{-1}; this is comparable to known rates for well-developed marshes [29]. These calculations are approximations of regional processes that demonstrate intimate connections between salt marsh hydrogeology, biogeochemistry, and C/N cycling (Figure 8).

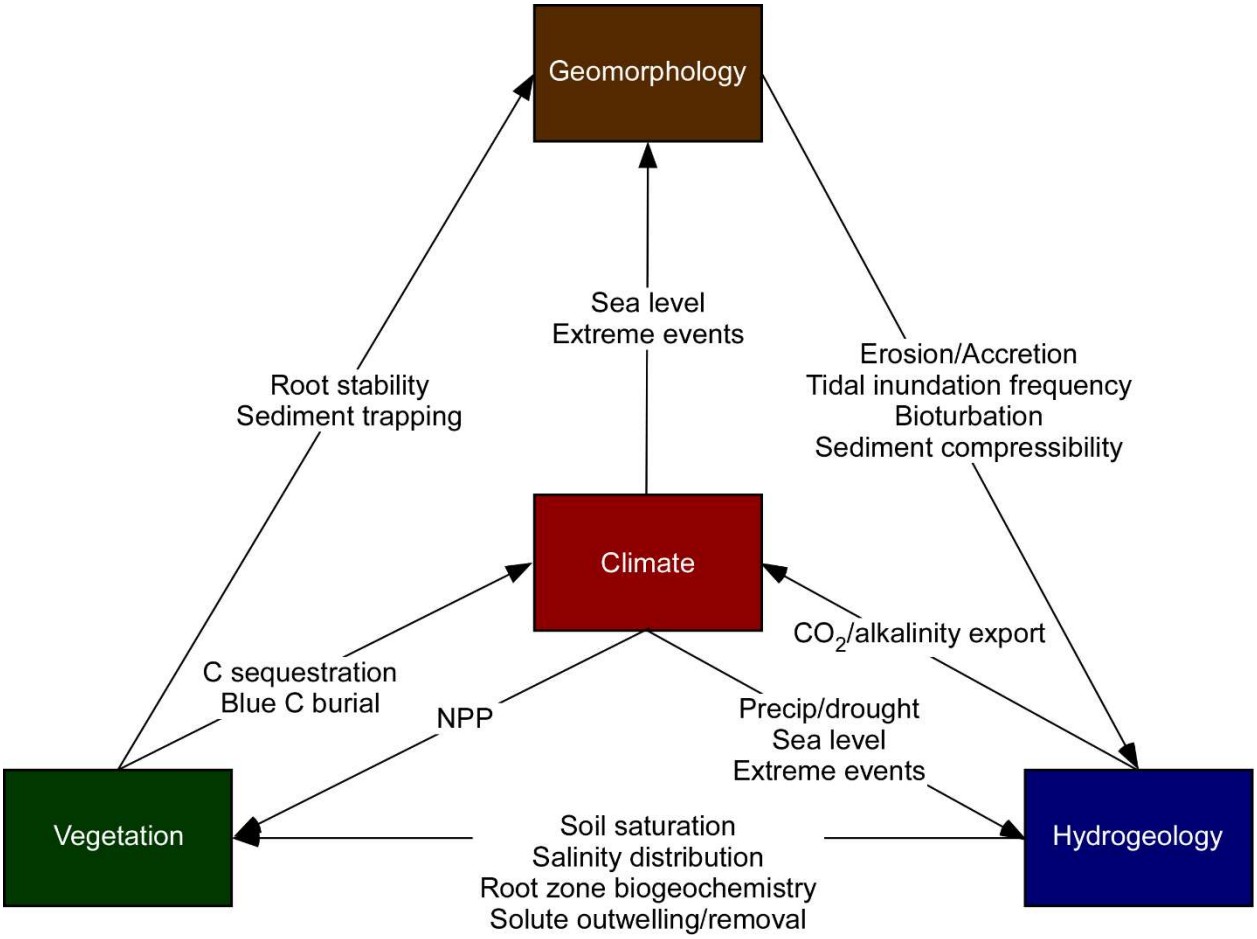

Figure 8. Generalized relationship of salt marsh ecosystem components including climate, geomorphology, hydrogeology and vegetation zonation. Note that human activities may impact each of these components with potential feedbacks outlined in the diagram. NPP = Net Primary Production; Precip = precipitation.

6. Targeted Questions

Multiple knowledge gaps were apparent from our synthesis of the salt marsh hydrogeology literature. Below we identify five critical questions that will not only contribute to enhanced system knowledge but will also inform management and coastal resilience strategies.

1. How do patterns and magnitudes of SGD and PEX vary across meso-, macro, and megatidal settings?

This question stems from the lack of diversity in settings in which PEX and SGD studies are conducted (microtidal US East Coast; Table 2). These biases increase uncertainty in upscaling as flux magnitudes are extrapolated across all tidal regimes. A more rigorous assessment of PEX and SGD across meso-, macro, and megatidal environments will help to confine uncertainty in regional-scale and global-scale estimates of PEX and SGD.

2. How does marsh PEX respond to extreme events?

Storm events may have immediate and longer-term effects on marsh PEX through changes in hydraulic gradients, salinity regimes, and sediment distributions. Depending on the event size or type (e.g., surge or precipitation dominated), shifts in flow regimes could last for days to months or longer. An understanding of storm impacts on PEX is essential for accurately estimating PEX and annual carbon exchange.

3. How will global climate change-induced marsh migration impact fluxes and the composition of PEX and SGD?

Located at the land–ocean margin, salt marshes are especially vulnerable to the effects of global climate change. For example, increased wave action is increasing edge erosion; sea level rise is threatening inundation; and changes in climate are altering temperature and precipitation regimes with impacts on vegetation. In response, marshes are transgressing landward; for many developed shorelines, marshes have no place to go. This landward transgression impacts the sediment composition, stratigraphy and topography of the marsh with unknown impacts on water and solute fluxes.

4. How do ecosystem components (e.g., climate, geomorphology, vegetation) impact PEX and SGD?

Salt marshes are complex ecosystems where climate, geomorphology, hydrogeology and vegetation are intricately linked (Figure 8). Factors that influence marsh PEX and SGD including recharge, hydraulic gradients, inundation frequency and sediment compressibility are all broadly affected by changes in climate, geomorphology and vegetation. Anthropogenic actions are an additional factor directly and indirectly impacting ecosystem function. Viewing any one of these ecosystem components independently may result in an oversimplification of the salt marsh ecosystem. Interdisciplinary assessments of these intricately linked ecosystem components are needed to help predict (1) future variability in marsh PEX and SGD, and (2) the resiliency of salt marshes to perturbations in global climate.

5. What are the links between ecosystem hydrogeology, water exchange, and carbon budgets?

Advances in blue carbon research are beginning to link marsh hydrogeology with carbon export to the ocean. The global significance of marsh PEX C export is unknown. Understanding the complex interactions between various ecosystem components (from questions 4) will not only help confine and upscale PEX, SGD, and carbon outwelling estimates but will also help inform management decisions in natural, managed, and restored marshes.

7. Summary and Conclusions

Porewater exchange (PEX) and submarine groundwater discharge (SGD) are unique processes in salt marshes that are individually impacted by drivers acting across multiple spatial and temporal scales. The delineation of these processes has enhanced our understanding of groundwater–surface water exchange in tidal marshes, yet the scope of knowledge is largely limited to microtidal marshes along the East Coast of the United States. There is a dire need for more PEX and SGD measurements from systems globally that transcend tidal ranges, geomorphological and topographic settings within marsh ecosystems. As we continue to conduct studies on salt marsh PEX and SGD, more descriptive characteristics need to be included and reported to establish relationships between marsh properties and water exchange magnitude. This includes, where appropriate, the marsh area and tidal channel length, marsh topography and hydroperiod, sediment characteristics (e.g., grain size, conductivity, peat thickness), stratigraphy, burrow density, vegetation type, and density and depth of the active root layer.

In an ideal study, multiple methods should be used to quantify marsh PEX and SGD. This includes well installation and logger deployment to qualitatively assess temporal dynamics across tidal cycles and seasons, and in response to extreme events. Seepage meters provide the only direct measurement of SGD and/or PEX; however, the labor required limits the temporal and spatial window captured. Radium-based approaches are integrative and can quantitatively separate PEX and SGD as a "snapshot" in time over a large area (e.g., embayment scale) or over tidal time scales at a single point in space (e.g., tidal creek). Numerical models provide an effective means to forecast future changes in marsh hydrogeology and will be an extremely important tool for predicting the impacts of continued climate change and sea level variability, in addition to marsh loss and transgression.

Lastly, we assert that future studies on salt marsh hydrogeology should be interdisciplinary to unravel the intertwined relationships between ecosystem components and

the resulting effects on PEX and SGD (Figure 8). The location and magnitude of marsh groundwater–surface water exchange can have a profound influence on vegetation zonation by influencing soil saturation, porewater salinity, and nutrient and trace element mobility and availability. In turn, changes in vegetation zonation impact marsh platform stability through sediment trapping and burial of organic material, and directly affects C sequestration and thus climate. Through interdisciplinary field campaigns that use multiple methods and reporting of descriptive site characteristics, we hope to enhance our present understanding and predictive capacity of global PEX and SGD, including their roles in nutrient, trace element, and carbon cycling and export.

Supplementary Materials: The following are available online at https://www.mdpi.com/2073-4441/13/4/543/s1. Summary of area-normalized marsh porewater and groundwater flux estimates, including methodology and relative time scales considered. Groundwater includes brackish and freshwater fluxes. Note that tidal range for each site is an approximation.

Author Contributions: J.G. and J.T. conceived, wrote, and edited this paper together. Both authors have read and agreed to the published version of this manuscript.

Funding: Seepage meter campaigns were funded by the Delaware Environmental Institute, the Delaware National Estuarine Research Reserve, and the National Science Foundation EAR-1759879. This research was in part funded by National Science Foundation grant number EAR-1759879.

Institutional Review Board Statement: Not applicable.

Informed Consent Statement: Not applicable.

Data Availability Statement: The seepage meter data presented in this study are openly available in Guimond, J. A. (2021). St. Jones NERR seepage meter field campaign data, HydroShare, https://doi.org/10.4211/hs.19b6a63d912b4a86aacc3a2aeb70558d.

Acknowledgments: Thank you to B. Kurylyk and H. Michael for providing helpful comments on an earlier version of this paper. We would also like to thank Carlos Duque Calvache and Xuan Yu for field assistance during seepage meter campaigns.

Conflicts of Interest: The authors declare no conflict of interest.

References

1. Moore, W.S. The Effect of Submarine Groundwater Discharge on the Ocean. *Annu. Rev. Mar. Sci.* **2010**, *2*, 59–88. [CrossRef]
2. Robinson, C.E.; Xin, P.; Santos, I.R.; Charette, M.A.; Li, L.; Barry, D. Groundwater dynamics in subterranean estuaries of coastal unconfined aquifers: Controls on submarine groundwater discharge and chemical inputs to the ocean. *Adv. Water Resour.* **2018**, *115*, 315–331. [CrossRef]
3. Taniguchi, M.; Dulai, H.; Burnett, K.M.; Santos, I.R.; Sugimoto, R.; Stieglitz, T.; Kim, G.; Moosdorf, N.; Burnett, W.C. Submarine Groundwater Discharge: Updates on Its Measurement Techniques, Geophysical Drivers, Magnitudes, and Effects. *Front. Environ. Sci.* **2019**, *7*, 1–26. [CrossRef]
4. Wang, Z.A.; Kroeger, K.D.; Ganju, N.K.; Gonneea, M.E.; Chu, S.N. Intertidal salt marshes as an important source of inorganic carbon to the coastal ocean. *Limnol. Oceanogr.* **2016**, *61*, 1916–1931. [CrossRef]
5. Najjar, R.G.; Herrmann, M.; Alexander, R.; Boyer, E.W.; Burdige, D.J.; Butman, D.; Cai, W.; Canuel, E.A.; Chen, R.F.; Friedrichs, M.A.M.; et al. Carbon Budget of Tidal Wetlands, Estuaries, and Shelf Waters of Eastern North America. *Glob. Biogeochem. Cycles* **2018**, *32*, 389–416. [CrossRef]
6. Tamborski, J.; Eagle, M.; Kurylyk, B.L.; Kroeger, K.; Wang, Z.A.; Henderson, P.; Charette, M.A. Porewater exchange driven inorganic carbon export from intertidal salt marshes. *Limnol. Oceanogr.* **2021**. [CrossRef]
7. Braswell, A.E.; Heffernan, J.B.; Kirwan, M.L. How Old Are Marshes on the East Coast, USA? Complex Patterns in Wetland Age Within and Among Regions. *Geophys. Res. Lett.* **2020**, *47*. [CrossRef]
8. Allen, J. Morphodynamics of Holocene salt marshes: A review sketch from the Atlantic and Southern North Sea coasts of Europe. *Quat. Sci. Rev.* **2000**, *19*, 1155–1231. [CrossRef]
9. Mitchell, M.; Herman, J.; Bilkovic, D.M.; Hershner, C. Marsh persistence under sea-level rise is controlled by multiple, geologically variable stressors. *Ecosyst. Heal. Sustain.* **2017**, *3*, 1379888. [CrossRef]
10. Perillo, G.M.E.; Wolanski, E.; Cahoon, D.R.; Hopkinson, C.S. (Eds.) *Coastal Wetlands: An Integrated Ecosystem Approach*, 2nd ed.; Elsevier: Amsterdam, The Netherlands, 2019.
11. Evans, T.B.; White, S.M.; Wilson, A.M. Coastal Groundwater Flow at the Nearshore and Embayment Scales: A Field and Modeling Study. *Water Resour. Res.* **2020**, *56*, 1–15. [CrossRef]

12. Moffett, K.B.; Gorelick, S.M.; McLaren, R.G.; Sudicky, E.A. Salt marsh ecohydrological zonation due to heterogeneous vegetation-groundwater-surface water interactions. *Water Resour. Res.* **2012**, *48*. [CrossRef]
13. Guimond, J.A.; Seyfferth, A.L.; Moffett, K.B.; Michael, H.A. A physical-biogeochemical mechanism for negative feedback between marsh crabs and carbon storage. *Environ. Res. Lett.* **2020**, *15*, 034024. [CrossRef]
14. Xiao, K.; Wilson, A.M.; Li, H.; Ryan, C. Crab burrows as preferential flow conduits for groundwater flow and transport in salt marshes: A modeling study. *Adv. Water Resour.* **2019**, *132*, 103408. [CrossRef]
15. Stumpf, R.P. The process of sedimentation on the surface of a salt marsh. *Estuar. Coast. Shelf Sci.* **1983**, *17*, 495–508. [CrossRef]
16. Harvey, J.W.; Nuttle, W.K. Fluxes of water and solute in a coastal wetland sediment. 2. Effect of macropores on solute exchange with surface water. *J. Hydrol.* **1995**, *164*, 109–125. [CrossRef]
17. Xin, P.; Yuan, L.-R.; Li, L.; Barry, D.A. Tidally driven multiscale pore water flow in a creek-marsh system. *Water Resour. Res.* **2011**, *47*, 1–19. [CrossRef]
18. Howes, B.; Goehringer, D. Porewater drainage and dissolved organic carbon and nutrient losses through the intertidal creek-banks of a New England salt marsh. *Mar. Ecol. Prog. Ser.* **1994**, *114*, 289–301. [CrossRef]
19. Seyfferth, A.L.; Bothfeld, F.; Vargas, R.; Stuckey, J.W.; Wang, J.; Kearns, K.; Michael, H.A.; Guimond, J.; Yu, X.; Sparks, D.L. Spatial and temporal heterogeneity of geochemical controls on carbon cycling in a tidal salt marsh. *Geochim. Cosmochim. Acta* **2020**, *282*, 1–18. [CrossRef]
20. Valiela, I.; Teal, J.M.; Volkmann, S.; Shafer, D.J.; Carpenter, E.J. Nutrient and particulate fluxes in a salt marsh ecosystem: Tidal exchanges and inputs by precipitation and groundwater 1. *Limnol. Oceanogr.* **1978**, *23*, 798–812. [CrossRef]
21. Dame, R.; Gardner, L. Nutrient processing and the development of tidal creek ecosystems. *Mar. Chem.* **1993**, *43*, 175–183. [CrossRef]
22. Teal, J.M. Energy Flow in the Salt Marsh Ecosystem of Georgia. *Ecol. Soc. Am.* **1962**, *43*, 614–624. [CrossRef]
23. Odum, E.P. Energy Flow in Ecosystems: A Historical Review. *Integr. Comp. Biol.* **1968**, *8*, 11–18. [CrossRef]
24. Whiting, G.J.; McKellar, H.N.; Spurrier, J.D.; Wolaver, T.G. Nitrogen exchange between a portion of vegetated salt marsh and the adjoining creek. *Limnol. Oceanogr.* **1989**, *34*, 463–473. [CrossRef]
25. Childers, D.; Day, J.W.; McKellar, H.N. Twenty more years of marsh and estuarine flux studies: Revisting Nixon (1980). In *Concepts and Controversies in Tidal Marsh Ecology*; Weinstein, D.A., Kreeger, M., Eds.; Kluwer Academic: Dordrecht, The Netherlands, 2000; pp. 391–424.
26. Krest, J.M.; Moore, W.S.; Gardner, L.R.; Morris, J.T. Marsh nutrient export supplied by groundwater discharge: Evidence from radium measurements. *Glob. Biogeochem. Cycles* **2000**, *14*, 167–176. [CrossRef]
27. Duarte, C.M.; Losada, I.J.; Hendriks, I.E.; Mazarrasa, I.; Marbà, N. The role of coastal plant communities for climate change mitigation and adaptation. *Nat. Clim. Chang.* **2013**, *3*, 961–968. [CrossRef]
28. Herrmann, M.; Najjar, R.G.; Kemp, W.M.; Alexander, R.B.; Boyer, E.W.; Cai, W.-J.; Griffith, P.C.; Kroeger, K.D.; McCallister, S.L.; Smith, R.A. Net ecosystem production and organic carbon balance of U.S. East Coast estuaries: A synthesis approach. *Glob. Biogeochem. Cycles* **2015**, *29*, 96–111. [CrossRef]
29. Tobias, C.; Neubauer, S.C. Salt Marsh Biogeochemistry: An overview. In *Coastal Wetlands: An Integrated Ecosystem Approach*; Elsevier Science: Amsterdam, The Netherlands, 2009; pp. 445–492.
30. Burnett, W.C.; Bokuniewicz, H.; Huettel, M.; Moore, W.S.; Taniguchi, M. Groundwater and pore water inputs to the coastal zone. *Biogeochemistry* **2003**, *66*, 3–33. [CrossRef]
31. Hemond, H.F.; Nuttle, W.K.; Burke, R.W.; Stolzenbach, K.D. Surface Infiltration in Salt Marshes: Theory, Measurement, and Biogeochemical Implications. *Water Resour. Res.* **1984**, *20*, 591–600. [CrossRef]
32. Harvey, J.W.; Germann, P.F.; Odum, W.E. Geomorphological control of subsurface hydrology in the creekbank zone of tidal marshes. *Estuar. Coast. Shelf Sci.* **1987**, *25*, 677–691. [CrossRef]
33. Nuttle, W.K.; Hemand, H.F. Salt marsh hydrology: Implications for biogeochemical fluxes to the atmosphere and estuaries. *Glob. Biogeochem. Cycles* **1988**, *2*, 91–114. [CrossRef]
34. Harvey, J.W.; Odum, W.E. The influence of tidal marshes on upland groundwater discharge to estuaries. *Biogeochemistry* **1990**, *10*, 217–236. [CrossRef]
35. Santos, I.R.; Eyre, B.D.; Huettel, M. The driving forces of porewater and groundwater flow in permeable coastal sediments: A review. *Estuar. Coast. Shelf Sci.* **2012**, *98*, 1–15. [CrossRef]
36. Nuttle, W.K.; Harvey, J.W. Fluxes of water and solute in a coastal wetland sediment. l. The contribution of regional groundwater discharge. *J. Hydrol.* **1995**, *164*, 89–107. [CrossRef]
37. Wilson, A.M.; Evans, T.; Moore, W.; Schutte, C.A.; Joye, S.B.; Hughes, A.H.; Anderson, J.L. Groundwater controls ecological zonation of salt marsh macrophytes. *Ecology* **2015**, *96*, 840–849. [CrossRef]
38. Tait, D.R.; Maher, D.T.; Macklin, P.A.; Santos, I.R. Mangrove pore water exchange across a latitudinal gradient. *Geophys. Res. Lett.* **2016**, *43*, 3334–3341. [CrossRef]
39. Santos, I.R.; Maher, D.T.; Larkin, R.; Webb, J.R.; Sanders, C.J. Carbon outwelling and outgassing vs. burial in an estuarine tidal creek surrounded by mangrove and saltmarsh wetlands. *Limnol. Oceanogr.* **2019**, *64*, 996–1013. [CrossRef]
40. Sadat-Noori, M.; Santos, I.R.; Tait, D.R.; Reading, M.J.; Sanders, C.J. High porewater exchange in a mangrove-dominated estuary revealed from short-lived radium isotopes. *J. Hydrol.* **2017**, *553*, 188–198. [CrossRef]

41. Tait, D.R.; Maher, D.T.; Sanders, C.J.; Santos, I.R. Radium-derived porewater exchange and dissolved N and P fluxes in mangroves. *Geochim. Cosmochim. Acta* **2017**, *200*, 295–309. [CrossRef]
42. Moffett, K.B.; Robinson, D.A.; Gorelick, S.M. Relationship of Salt Marsh Vegetation Zonation to Spatial Patterns in Soil Moisture, Salinity, and Topography. *Ecosystems* **2010**, *13*, 1287–1302. [CrossRef]
43. Silvestri, S.; Defina, A.; Marani, M. Tidal regime, salinity and salt marsh plant zonation. *Estuar. Coast. Shelf Sci.* **2005**, *62*, 119–130. [CrossRef]
44. Xin, P.; Kong, J.; Li, L.; Barry, D. Modelling of groundwater–vegetation interactions in a tidal marsh. *Adv. Water Resour.* **2013**, *57*, 52–68. [CrossRef]
45. Michael, H.A.; Mulligan, A.E.; Harvey, C.F. Seasonal oscillations in water exchange between aquifers and the coastal ocean. *Nature* **2005**, *436*, 1145–1148. [CrossRef]
46. Zhang, Y.; Li, W.; Sun, G.; Miao, G.; Noormets, A.; Emanuel, R.; King, J.S. Understanding coastal wetland hydrology with a new regional-scale, process-based hydrological model. *Hydrol. Process.* **2018**, *32*, 3158–3173. [CrossRef]
47. Lapo, K.E.; Hinkelman, L.M.; Raleigh, M.S.; Lundquist, J.D. What time scales are important for monitoring tidally influenced submarine groundwater discharge? Insights from a salt marsh. *Water Resour. Res.* **2015**, *51*, 1649–1670. [CrossRef]
48. Wilson, A.M.; Moore, W.S.; Joye, S.B.; Anderson, J.L.; Schutte, C.A. Storm-driven groundwater flow in a salt marsh. *Water Resour. Res.* **2011**, *47*, 1–11. [CrossRef]
49. Peterson, R.N.; Meile, C.; Peterson, L.E.; Carter, M.; Miklesh, D. Groundwater discharge dynamics into a salt marsh tidal river. *Estuar. Coast. Shelf Sci.* **2019**, *218*, 324–333. [CrossRef]
50. Wilson, A.M.; Gardner, L.R. Tidally driven groundwater flow and solute exchange in a marsh: Numerical simulations. *Water Resour. Res.* **2006**, *42*, 1–9. [CrossRef]
51. Xin, P.; Zhou, T.; Lu, C.; Shen, C.; Zhang, C.; D'Alpaos, A.; Li, L. Combined effects of tides, evaporation and rainfall on the soil conditions in an intertidal creek-marsh system. *Adv. Water Resour.* **2017**, *103*, 1–15. [CrossRef]
52. Ursino, N.; Silvestri, S.; Marani, M. Subsurface flow and vegetation patterns in tidal environments. *Water Resour. Res.* **2004**, *40*, 1–11. [CrossRef]
53. Li, L.; Barry, D.A.; Stagnitti, F.; Parlange, J.-Y. Submarine groundwater discharge and associated chemical input to a coastal sea. *Water Resour. Res.* **1999**, *35*, 3253–3259. [CrossRef]
54. Wilson, A.M.; Morris, J.T. The influence of tidal forcing on groundwater flow and nutrient exchange in a salt marsh-dominated estuary. *Biogeochemistry* **2012**, *108*, 27–38. [CrossRef]
55. Bollinger, M.; Moore, W. Evaluation of salt marsh hydrology using radium as a tracer. *Geochim. Cosmochim. Acta* **1993**, *57*, 2203–2212. [CrossRef]
56. Wilson, C.; Hughes, Z.; Fitzgerald, D. The effects of crab bioturbation on Mid-Atlantic saltmarsh tidal creek extension: Geotechnical and geochemical changes. *Estuar. Coast. Shelf Sci.* **2012**, *106*, 33–44. [CrossRef]
57. Zhou, T.; Xin, P.; Li, L.; Barry, D.; Šimůnek, J. Effects of large macropores on soil evaporation in salt marshes. *J. Hydrol.* **2020**, *584*, 124754. [CrossRef]
58. Katz, L.C. Effects of burrowing by the fiddler crab, Uca pugnax (Smith). *Estuar. Coast. Mar. Sci.* **1980**, *11*, 233–237. [CrossRef]
59. McCraith, B.J.; Gardner, L.R.; Wethey, D.S.; Moore, W.S. The effect of fiddler crab burrowing on sediment mixing and radionuclide profiles along a topographic gradient in a southeastern salt marsh. *J. Mar. Res.* **2003**, *61*, 359–390. [CrossRef]
60. Xin, P.; Jin, G.; Li, L.; Barry, D. Effects of crab burrows on pore water flows in salt marshes. *Adv. Water Resour.* **2009**, *32*, 439–449. [CrossRef]
61. Gonneea, M.E.; Mulligan, A.E.; Charette, M.A. Climate-driven sea level anomalies modulate coastal groundwater dynamics and discharge. *Geophys. Res. Lett.* **2013**, *40*, 2701–2706. [CrossRef]
62. Guimond, J.A.; Yu, X.; Seyfferth, A.L.; Michael, H.A. Using Hydrological-Biogeochemical Linkages to Elucidate Carbon Dynamics in Coastal Marshes Subject to Relative Sea Level Rise. *Water Resour. Res.* **2020**, *56*, 1–16. [CrossRef]
63. Wasson, K.; Raposa, K.; Almeida, M.; Beheshti, K.; Crooks, J.A.; Deck, A.; Dix, N.; Garvey, C.; Goldstein, J.; Johnson, D.S.; et al. Pattern and scale: Evaluating generalities in crab distributions and marsh dynamics from small plots to a national scale. *Ecology* **2019**, *100*, e02813. [CrossRef]
64. Rosenberry, D.O.; Duque, C.; Lee, D.R. History and evolution of seepage meters for quantifying flow between groundwater and surface water: Part 1—Freshwater settings. *Earth-Sci. Rev.* **2020**, *204*, 103167. [CrossRef]
65. Duque, C.; Russoniello, C.J.; Rosenberry, D.O. History and evolution of seepage meters for quantifying flow between groundwater and surface water: Part 2—Marine settings and submarine groundwater discharge. *Earth-Sci. Rev.* **2020**, *204*, 103168. [CrossRef]
66. Lee, D.R. A device for measuring seepage flux in lakes and estuaries1. *Limnol. Oceanogr.* **1977**, *22*, 140–147. [CrossRef]
67. Paulsen, R.J.; Smith, C.F.; O'Rourke, D.; Wong, T.-F. Development and Evaluation of an Ultrasonic Ground Water Seepage Meter. *Ground Water* **2001**, *39*, 904–911. [CrossRef]
68. Taniguchi, M.; Fukuo, Y. Continuous Measurements of Ground-Water Seepage Using an Automatic Seepage Meter. *Ground Water* **1993**, *31*, 675–679. [CrossRef]
69. Sholkovitz, E.; Herbold, C.; Charette, M. An automated dye-dilution based seepage meter for the time-series measurement of submarine groundwater discharge. *Limnol. Oceanogr. Methods* **2003**, *1*, 16–28. [CrossRef]
70. Rosenberry, D.O.; LaBaugh, J.W. Field Techniques for Estimating Water Fluxes between Surface Water and Ground Water. *U.S. Geol. Surv.* **2008**, 128. [CrossRef]

71. Whiting, G.J.; Childers, D.L. Subtidal advective water flux as a potentially important nutrient input to southeastern U.S.A. Saltmarsh estuaries. *Estuar. Coast. Shelf Sci.* **1989**, *28*, 417–431. [CrossRef]
72. Gardner, L.R. A modeling study of the dynamics of pore water seepage from intertidal marsh sediments. *Estuar. Coast. Shelf Sci.* **2005**, *62*, 691–698. [CrossRef]
73. Burnett, W.; Aggarwal, P.; Aureli, A.; Bokuniewicz, H.; Cable, J.; Charette, M.; Kontar, E.; Krupa, S.; Kulkarni, K.; Loveless, A.; et al. Quantifying submarine groundwater discharge in the coastal zone via multiple methods. *Sci. Total Environ.* **2006**, *367*, 498–543. [CrossRef]
74. Cable, J.; Burnett, W.; Chanton, J.; Corbett, D.; Cable, P. Field Evaluation of Seepage Meters in the Coastal Marine Environment. *Estuar. Coast. Shelf Sci.* **1997**, *45*, 367–375. [CrossRef]
75. Russoniello, C.J.; Michael, H.A. Investigation of Seepage Meter Measurements in Steady Flow and Wave Conditions. *Ground Water* **2014**, *53*, 959–966. [CrossRef] [PubMed]
76. Bouwer, H.; Rice, R.C. A slug test for determining hydraulic conductivity of unconfined aquifers with completely or partially penetrating wells. *Water Resour. Res.* **1976**, *12*, 423–428. [CrossRef]
77. Byers, S.E.; Chmura, G.L. Observations on Shallow Subsurface Hydrology at Bay of Fundy Macrotidal Salt Marshes. *J. Coast. Res.* **2014**, *297*, 1006–1016. [CrossRef]
78. Xiao, K.; Wilson, A.M.; Li, H.; Santos, I.R.; Tamborski, J.; Smith, E.; Lang, S.Q.; Zheng, C.; Luo, X.; Lu, M.; et al. Large CO_2 release and tidal flushing in salt marsh crab burrows reduce the potential for blue carbon sequestration. *Limnol. Oceanogr.* **2020**, *66*, 14–29. [CrossRef]
79. Chen, X. Measurement of streambed hydraulic conductivity and its anisotropy. *Environ. Earth Sci.* **2000**, *39*, 1317–1324. [CrossRef]
80. Schultz, G.; Ruppel, C. Constraints on hydraulic parameters and implications for groundwater flux across the upland–estuary interface. *J. Hydrol.* **2002**, *260*, 255–269. [CrossRef]
81. Freeze, R.A.; Cherry, J.A. *Groundwater*; Prentice-Hall: Englewood Cliffs, NJ, USA, 1979.
82. Gardner, L.R. Assessing the accuracy of monitoring wells in tidal wetlands. *Water Resour. Res.* **2009**, *45*, 1–5. [CrossRef]
83. Gardner, L.R.; Gaines, E.F. A method for estimating pore water drainage from marsh soils using rainfall and well records. *Estuar. Coast. Shelf Sci.* **2008**, *79*, 51–58. [CrossRef]
84. Tobias, C.R.; Harvey, J.W.; Anderson, I.C. Quantifying groundwater discharge through fringing wetlands to estuaries: Seasonal variability, methods comparison, and implications for wetland-estuary exchange. *Limnol. Oceanogr.* **2001**, *46*, 604–615. [CrossRef]
85. Drexler, J.Z.; Snyder, R.L.; Spano, D.; Paw U, K.T. A review of models and micrometeorological methods used to estimate wetland evapotranspiration. *Hydrol. Process.* **2004**, *18*, 2071–2101. [CrossRef]
86. Gardner, L.R. Role of geomorphic and hydraulic parameters in governing pore water seepage from salt marsh sediments. *Water Resour. Res.* **2005**, *41*. [CrossRef]
87. Shen, C.; Zhang, C.; Jin, G.; Kong, J.; Li, L. Effects of unstable flow on solute transport in the marsh soil and exchange with coastal water. *Geophys. Res. Lett.* **2016**, *43*, 1–11. [CrossRef]
88. Xiao, K.; Li, H.; Xia, Y.; Yang, J.; Wilson, A.M.; Michael, H.A.; Geng, X.; Smith, E.; Boufadel, M.C.; Yuan, P.; et al. Effects of Tidally Varying Salinity on Groundwater Flow and Solute Transport: Insights From Modelling an Idealized Creek Marsh Aquifer. *Water Resour. Res.* **2019**, *55*, 9656–9672. [CrossRef]
89. Yuan, L.-R.; Xin, P.; Kong, J.; Li, L.; Lockington, D. A coupled model for simulating surface water and groundwater interactions in coastal wetlands. *Hydrol. Process.* **2011**, *25*, 3533–3546. [CrossRef]
90. Gardner, L.R.; Wilson, A.M. Comparison of four numerical models for simulating seepage from salt marsh sediments. *Estuar. Coast. Shelf Sci.* **2006**, *69*, 427–437. [CrossRef]
91. Reeves, H.W.; Thibodeau, P.M.; Underwood, R.G.; Gardner, L.R. Incorporation of Total Stress Changes into the Ground Water Model SUTRA. *Ground Water* **2000**, *38*, 89–98. [CrossRef]
92. Shen, C.; Zhang, C.; Xin, P.; Kong, J.; Li, L. Salt Dynamics in Coastal Marshes: Formation of Hypersaline Zones. *Water Resour. Res.* **2018**, *54*, 3259–3276. [CrossRef]
93. Moffett, K.B.; Wolf, A.; Berry, J.A.; Gorelick, S.M. Salt marsh–atmosphere exchange of energy, water vapor, and carbon dioxide: Effects of tidal flooding and biophysical controls. *Water Resour. Res.* **2010**, *46*, 1–18. [CrossRef]
94. Moffett, K.B.; Gorelick, S.M. A method to calculate heterogeneous evapotranspiration using submeter thermal infrared imagery coupled to a stomatal resistance submodel. *Water Resour. Res.* **2012**, *48*, 1–18. [CrossRef]
95. Swarzenski, P.W. U/Th Series Radionuclides as Coastal Groundwater Tracers. *Chem. Rev.* **2007**, *107*, 663–674. [CrossRef] [PubMed]
96. Charette, M.; Moore, W.; Burnett, W. Uranium- and thorium-series nuclides as tracers of submarine groundwater discharge. In *U-Th Series Nuclides in Aquatic Systems*; Elsevier: Amsterdam, The Netherlands, 2008; pp. 155–191.
97. Bollinger, M.S.; Moore, W.S. Radium fluxes from a salt marsh. *Nature.* **1984**, *309*, 444–446. [CrossRef]
98. Rama; Moore, W.S. Using the radium quartet for evaluating groundwater input and water exchange in salt marshes. *Geochim. Cosmochim. Acta* **1996**, *60*, 4645–4652. [CrossRef]
99. Krest, J.M.; Harvey, J.W. Using natural distributions of short-lived radium isotopes to quantify groundwater discharge and recharge. *Limnol. Oceanogr.* **2003**, *48*, 290–298. [CrossRef]
100. Michael, H.A.; Charette, M.A.; Harvey, C.F. Patterns and variability of groundwater flow and radium activity at the coast: A case study from Waquoit Bay, Massachusetts. *Mar. Chem.* **2011**, *127*, 100–114. [CrossRef]

101. Tamborski, J.J.; Cochran, J.K.; Heilbrun, C.; Rafferty, P.; Fitzgerald, P.; Zhu, Q.; Salazar, C. Investigation of pore water residence times and drainage velocities in salt marshes using short-lived radium isotopes. *Mar. Chem.* **2017**, *196*, 107–115. [CrossRef]
102. Cai, P.; Shi, X.; Moore, W.S.; Dai, M. Measurement of ^{224}Ra:^{228}Th disequilibrium in coastal sediments using a delayed coincidence counter. *Mar. Chem.* **2012**, *138–139*, 1–6. [CrossRef]
103. Shi, X.; Benitez-Nelson, C.R.; Cai, P.; He, L.; Moore, W.S. Development of a two-layer transport model in layered muddy-permeable marsh sediments using ^{224}Ra-^{228}Th disequilibria. *Limnol. Oceanogr.* **2019**, *64*, 1672–1687. [CrossRef]
104. Shi, X.; Mason, R.P.; Charette, M.A.; Mazrui, N.M.; Cai, P. Mercury flux from salt marsh sediments: Insights from a comparison between ^{224}Ra/^{228}Th disequilibrium and core incubation methods. *Geochim. Cosmochim. Acta* **2018**, *222*, 569–583. [CrossRef]
105. Dias, D.M.C.; Copeland, J.M.; Milliken, C.L.; Shi, X.; Ferry, J.L.; Shaw, T.J. Production of Reactive Oxygen Species in the Rhizosphere of a Spartina-Dominated Salt Marsh Systems. *Aquat. Geochem.* **2016**, *22*, 573–591. [CrossRef]
106. Charette, M.A.; Splivallo, R.; Herbold, C.; Bollinger, M.S.; Moore, W.S. Salt marsh submarine groundwater discharge as traced by radium isotopes. *Mar. Chem.* **2003**, *84*, 113–121. [CrossRef]
107. Schutte, C.A.; Moore, W.S.; Wilson, A.M.; Joye, S.B. Groundwater-Driven Methane Export Reduces Salt Marsh Blue Carbon Potential. *Glob. Biogeochem. Cycles* **2020**, *34*, 1–16. [CrossRef]
108. Beck, A.J.; Rapaglia, J.P.; Cochran, J.K.; Bokuniewicz, H.J. Radium mass-balance in Jamaica Bay, NY: Evidence for a substantial flux of submarine groundwater. *Mar. Chem.* **2007**, *106*, 419–441. [CrossRef]
109. Charette, M.A. Hydrologic forcing of submarine groundwater discharge: Insight from a seasonal study of radium isotopes in a groundwater-dominated salt marsh estuary. *Limnol. Oceanogr.* **2007**, *52*, 230–239. [CrossRef]
110. Charette, M.A.; Buesseler, K.O. Submarine groundwater discharge of nutrients and copper to an urban subestuary of Chesapeake Bay (Elizabeth River). *Limnol. Oceanogr.* **2004**, *49*, 376–385. [CrossRef]
111. Gleeson, J.; Santos, I.R.; Maher, D.T.; Golsby-Smith, L. Groundwater–surface water exchange in a mangrove tidal creek: Evidence from natural geochemical tracers and implications for nutrient budgets. *Mar. Chem.* **2013**, *156*, 27–37. [CrossRef]
112. Xiao, K.; Li, H.; Wilson, A.M.; Xia, Y.; Wan, L.; Zheng, C.; Ma, Q.; Wang, C.; Wang, X.; Jiang, X. Tidal groundwater flow and its ecological effects in a brackish marsh at the mouth of a large sub-tropical river. *J. Hydrol.* **2017**, *555*, 198–212. [CrossRef]
113. Giblin, A.E.; Gaines, A.G. Nitrogen inputs to a marine embayment: The importance of groundwater. *Biogeochemistry* **1990**, *10*, 309–328. [CrossRef]
114. Hemond, H.F.; Fifield, J.L. Subsurface flow in salt marsh peat: A model and field study1. *Limnol. Oceanogr.* **1982**, *27*, 126–136. [CrossRef]
115. Lee, D.R. Groundwater-solute influx. *Limnol. Oceanogr.* **1980**, *25*, 183–186. [CrossRef]
116. Valiela, I.; Teal, J.M.; Volkmann, S.B.; Cogswell, C.M.; Harrington, R.A. On the measurement of tidal exchanges and groundwater flow in salt marshes. *Limnol. Oceanogr.* **1980**, *25*, 187–192. [CrossRef]
117. Osgood, D.T. Subsurface hydrology and nutrient export from barrier island marshes at different tidal ranges. *Wetl. Ecol. Manag.* **2000**, *8*, 133–146. [CrossRef]
118. Morris, J.T. The Mass Balance of Salt and Water in Intertidal Sediments: Results from North Inlet, South Carolina. *Estuaries* **1995**, *18*, 556–567. [CrossRef]
119. Bradley, P.M.; Morris, J.T. Physical characteristics of salt marsh sediments: Ecological implications. *Mar. Ecol. Prog. Ser.* **1990**, *61*, 245–252. [CrossRef]
120. Webb, J.R.; Santos, I.R.; Maher, D.T.; Tait, D.R.; Cyronak, T.; Sadat-Noori, M.; Macklin, P.; Jeffrey, L.C. Groundwater as a source of dissolved organic matter to coastal waters: Insights from radon and CDOM observations in 12 shallow coastal systems. *Limnol. Oceanogr.* **2019**, *64*, 182–196. [CrossRef]
121. Qu, W.; Li, H.; Huang, H.; Zheng, C.; Wang, C.; Wang, X.; Zhang, Y. Seawater-groundwater exchange and nutrients carried by submarine groundwater discharge in different types of wetlands at Jiaozhou Bay, China. *J. Hydrol.* **2017**, *555*, 185–197. [CrossRef]
122. Befus, K.M.; Kroeger, K.D.; Smith, C.G.; Swarzenski, P.W. The Magnitude and Origin of Groundwater Discharge to Eastern U.S. and Gulf of Mexico Coastal Waters. *Geophys. Res. Lett.* **2017**, *44*, 1–11. [CrossRef]
123. Hinson, A.L.; Feagin, R.A.; Eriksson, M.; Najjar, R.G.; Herrmann, M.; Bianchi, T.S.; Kemp, M.; Hutchings, J.A.; Crooks, S.; Boutton, T. The spatial distribution of soil organic carbon in tidal wetland soils of the continental United States. *Glob. Chang. Biol.* **2017**, *23*, 5468–5480. [CrossRef]
124. Emery, K. Hypsometry of the continental shelf off eastern North America. *Estuar. Coast. Mar. Sci.* **1979**, *9*, 653–658. [CrossRef]
125. Porubsky, W.; Weston, N.B.; Moore, W.S.; Ruppel, C.D.; Joye, S.B. Dynamics of submarine groundwater discharge and associated fluxes of dissolved nutrients, carbon, and trace gases to the coastal zone (Okatee River estuary, South Carolina). *Geochim. Cosmochim. Acta* **2014**, *131*, 81–97. [CrossRef]